Received: 18 August 2016 | Revised: 15 November 2016 | Accepted: 16 November 2016

DOI 10.1002/eco.1815

WILEY

RESEARCH ARTICLE

Contrasting strategies of hydraulic control in two codominant temperate tree species

Ashley M. Matheny[1] | Richard P. Fiorella[2,3] | Gil Bohrer[1] | Christopher J. Poulsen[2] | Timothy H. Morin[1] | Alyssa Wunderlich[1] | Christoph S. Vogel[4] | Peter S. Curtis[5]

[1] Department of Civil, Environmental, and Geodetic Engineering, The Ohio State University, Columbus, OH 43210, USA

[2] Department of Earth and Environmental Sciences, University of Michigan, Ann Arbor, MI 48109, USA

[3] Department of Geology and Geophysics, University of Utah, Salt Lake City, UT 84112, USA

[4] University of Michigan Biological Station, Pellston, MI 49769, USA

[5] Department of Evolution, Ecology, and Organismal Biology, The Ohio State University, Columbus, OH 43210, USA

Correspondence
Ashley M. Matheny, Department of Civil, Environmental, and Geodetic Engineering, The Ohio State University, Columbus, OH 43210, USA.
Email: matheny.44@osu.edu

Funding information
National Science Foundation Hydrological Science, Grant/Award Number: 1521238; Lawrence Berkeley National Laboratory; Ameriflux Management program under Flux Core Site Agreement, Grant/Award Number: 7096915; U.S. Department of Energy's Office of Science, Office of Biological and Environmental Research, Terrestrial Ecosystem Sciences Program Award, Grant/Award Number: DE-SC0007041

Abstract

Biophysical controls on plant water status exist at the leaf, stem, and root levels. Therefore, we pose that hydraulic strategy is a combination of traits governing water use at each of these three levels. We studied sap flux, stem water storage, stomatal conductance, photosynthesis, and growth of red oaks (*Quercus rubra*) and red maples (*Acer rubrum*). These species differ in stomatal hydraulic strategy and xylem architecture and may root at different depths. Stable isotope analysis of xylem water was used to identify root water uptake depth. Oaks were shown to access a deeper water source than maples. During non-limiting soil moisture conditions, transpiration was greater in maples than in oaks. However, during a soil dry down, transpiration and stem water storage decreased by more than 80% and 28% in maples but only by 31% and 1% in oaks. We suggest that the preferential use of deep water by red oaks allows the species to continue transpiration and growth during soil water limitations. In this case, deeper roots may provide a buffer against drought-induced mortality. Using 14 years of growth data, we show that maple growth correlates with mean annual soil moisture at 30 cm but oak growth does not. The observed responses of oak and maple to drought were not able to be explained by leaf and xylem physiology alone. We employed the Finite-difference Ecosystem-scale Tree Crown Hydrodynamics model version 2 plant hydrodynamics model to demonstrate the influence of root, stem, and leaf controls on tree-level transpiration. We conclude that all three levels of hydraulic traits are required to define hydraulic strategy.

KEYWORDS

Acer rubrum, hydraulic strategy, plant functional type, plant-hydrodynamics model, *Quercus rubra*, sap flux, stable isotope analysis, stem water storage

1 | INTRODUCTION

Water availability limits transpiration and carbon uptake in plants (Dawson, 1993; Horton & Hart, 1998). Plants regulate water status dynamically through controls at the leaf, stem, and root levels. At the leaf level, stomata can close during water stress to maintain a steady, high leaf water potential (isohydry); remain open while risking highly negative leaf water potentials to maximize carbon uptake (anisohydry); or operate along a range of intermediate strategies (McDowell et al., 2008; Skelton, West, & Dawson, 2015). At the stem level, conductive woody tissue differs in the size and organization of conductive xylem vessels, leading to differences in maximum conductivity (high vs. low) and the water pressure at which the onset of cavitation occurs (cavitation-resistant xylem vs. cavitation-vulnerable xylem). Conductivity and vulnerability typically correlate with the morphology of the xylem, with ring-porous xylem tending to be more conductive but more cavitation vulnerable, and diffuse-porous xylem with lower maximum conductivity but less cavitation vulnerable (Pockman & Sperry, 2000). Conifers present a tracheid-based morphology that may be more cavitation resistant than both angiosperm wood types and have lower hydraulic conductivity than diffuse-porous xylem (Sperry, Nichols, Sullivan, & Eastlack, 1994; Choat et al., 2012). A third axis of hydraulic control results from the architecture of root systems across different species. Species with deeper roots can access water at greater depths than

are unavailable to more shallowly rooted species (Jackson et al., 1996; Canadell et al., 1996). Different species exhibit a spectrum of traits that vary in cavitation risk across all three of these axes of hydraulic control (Figure 1; Meinzer, Woodruff, Marias, McCulloh, & Sevanto, 2014).

Regulation of water use is often considered to be primarily dominated by interactions between xylem architecture and stomatal behavior (McDowell et al., 2008). In many cases, vascular structure and stomatal response strategies may covary to optimize water use and offset risks associated with traits along the other axis (Manzoni, 2014; Manzoni, Vico, Katul, Palmroth, & Porporato, 2014; Nolf et al., 2015). However, several counterexamples exist. For example, many species of trees operate stomata anisohydrically, despite having more vulnerable ring-porous xylem (Martinez-Vilalta, Poyatos, Aguade, Retana, & Mencuccini, 2014; Thomsen et al., 2013). Yet, these trees rarely experience hydraulic limitations to transpiration and some are quite drought resistant (Cochard, Breda, Granier, & Aussenac, 1992). Therefore, the combination of leaf and xylem traits may not be sufficient to explain plant water-use dynamics. This portends that root-level controls must also be considered to understand plant water use and drought susceptibility. We term the syndrome of emergent phenotypic hydraulic functional traits at the root, stem, and leaf levels as the whole-plant hydraulic strategy and posit its governing role in not only plant-level water use but also ecosystem-level water use (Matheny, Mirfenderesgi, & Bohrer, 2016).

Differences among species in whole-plant hydraulic strategy promote distinct transpiration rates and patterns (Dawson, 1993; Dawson, 1996; Meinzer et al., 1999; Nadezhdina, Ferreira, Silva, & Pacheco, 2008; McCulloh et al., 2012; Ford, Hubbard, & Vose, 2011). It is common for species within the same ecosystem to employ opposing hydraulic strategies (e.g., risk prone or risk adverse; McCulloh et al., 2012; Ford et al., 2011). Disparities in transpiration volume and timing, due to differences in whole-plant hydraulic strategies employed within the same forest, have important implications for forest growth and response to drought and disturbance (Roman et al., 2015; McDowell et al., 2008; Matheny et al., 2014b; Gao et al., 2015; Gu, Pallardy, Hosman, & Sun, 2015; Wullschleger, Meinzer, & Vertessy, 1998). Several water flux studies have shown that many species of ring-porous, anisohydric oak continue to transpire after other species curtail their water use during mild to moderate drought (e.g., von Allmen, Sperry, & Bush, 2014; Baldocchi & Xu, 2007; Hernandez-Santana, Martinez-Fernandez, Moran, & Cano, 2008; Matheny et al., 2014b). To explain this observation, we suggest that certain species of oaks may root more deeply than co-occurring species and therefore may access water pools that are unavailable to other species. Although only a limited number of studies have looked directly into the relationship between oak root-water uptake depth and transpiration, a few have shown the importance of deep water access for drought resistance (Miller, Chen, Rubin, Ma, & Baldocchi, 2010; Nadezhdina et al., 2008; Pinto et al., 2014; Phillips & Ehleringer, 1995). Traits within the rhizosphere such as rooting depth and vertical distribution, root length and diameter distribution, root water uptake efficiency, and mycorrhizal interaction have been shown to influence water acquisition and use (Matheny et al., 2016; Canadell, Pataki, & Pitelka, 2007; Allen, 2009).The hypothesized "safe" rooting strategy of oaks may be the key that permits the high-risk combination of anisohydry and ring-porous xylem in terms of the proposed plant hydraulic safety–efficiency trade-off (Meinzer, McCulloh, Lachenbruch, Woodruff, & Johnson, 2010; Manzoni et al., 2013, but see the counter arguement presented by Gleason et al. 2016). Deep roots may also be the critical aspect of hydraulic strategy that provides additional drought resilience to oak-dominated ecosystems (Tognetti, Longobucco, & Raschi, 1998).

In a study of species-specific water relations, anisohydric, ring-porous red oak (*Quercus rubra* L.) did not demonstrate the water-stress-induced limitations to transpiration expected for this combination of risk-prone hydraulic traits (Matheny et al., 2014b). For the same field site, Thomsen et al. (2013) showed that red maple (*Acer rubrum* L.) exhibited an "ultra" safe strategy combining isohydric stomatal regulation with diffuse-porous xylem. Both studies postulate that the observed sustained transpiration by red oaks during water stress may result from a deep rooting strategy. Here, we examine the effects of potential rooting depth differences between red oaks and red maples using stable isotope analysis of xylem water from both species. Stable xylem water isotopes are useful tracers because they reflect the isotopic composition of source water taken up by the roots (Walker & Richardson, 1991; Ehleringer & Dawson, 1992). Phase changes associated with precipitation and evaporation unequally partition the heavy and light isotopes of oxygen and hydrogen in water, promoting distinct isotope values across different environmental water sources (Ehleringer & Dawson, 1992; West et al., 2012; Gaines et al., 2015; Gat, 1996). We integrate our isotopic analysis with measurements of sap flow, stomatal conductance, photosynthesis, and long-term growth to compare the performance of these two species with respect to each of the three compartments of the whole-plant hydraulic strategy.

We use a tree-level hydrodynamic modeling framework to test the sensitivity of whole-plant transpiration to different components of the hydraulic regulation system, inclusive of different combinations of root, stem, and leaf traits on transpiration. This type of trait-based approach to describing hydraulic strategy at the species-level could

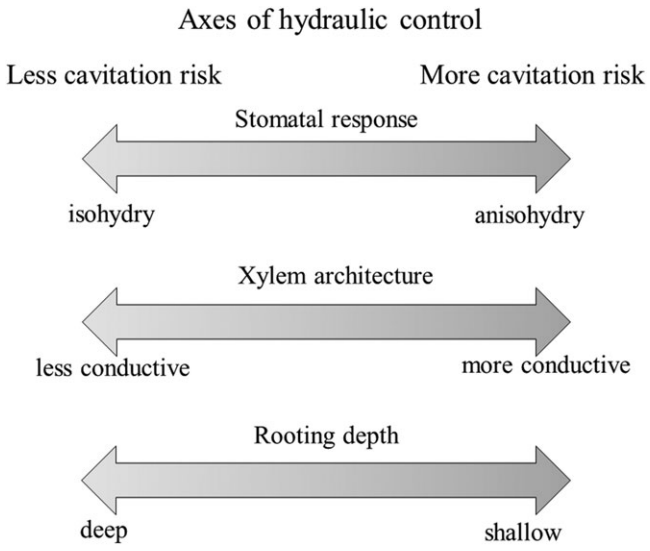

FIGURE 1 Schematic diagram of risk levels associated with hydraulic strategy at each of the three levels of plant hydraulic control

potentially inform the representation of plant hydraulic function within plant-functional types in ecosystem and land-surface models (Matheny et al., 2016). It has been shown that over-aggregation of functionally distinct species, such as red oak and red maple, into the same plant functional type (e.g., temperate broadleaf deciduous) leads to errors in short- and long-term predictions of water and carbon fluxes (Poulter et al., 2011; Matheny et al., 2014a; Matthes, Goring, Williams, & Dietze, 2016). Recent efforts to include plant hydraulic traits and the resultant hydrodynamics in ecosystem models have shown promise for improving simulations of transpiration and alleviating some of these errors (Xu, Medvigy, Powers, Becknell, & Guan, 2016).

We hypothesize that (1) red oaks in northern Michigan are rooted more deeply than red maples and therefore can access a steady and deep supply of water that red maples cannot. (2) This deep and steady water supply permits red oaks to maintain transpiration when soil moisture within the top 3 m of the soil is depleted. (3) We expect that bole growth will be closely coupled with surficial soil moisture (30 cm) in species whose overall transpiration is more limited by hydraulic stress, such as red maples, but not red oaks. (4) We predict that each combination of leaf, stem, and root traits comprising different whole-plant hydraulic strategies, will lead to different transpiration rates and will be sensitive to hydraulic limitations under different ranges of environmental water stress.

2 | MATERIALS AND METHODS

2.1 | Site description

This study was conducted within the footprint of the Ameriflux-affiliated eddy covariance tower, US-UMB (45° 33′ 35″ N, 84° 42′ 48″ W, elev. 236 m) at the University of Michigan Biological Station (UMBS) in northern lower Michigan, USA. The 30-year mean annual precipitation for the region is 766 mm with a mean annual temperature of 5.5 °C (Pellston, MI Regional Airport, NOAA National Climate Data Center). Local soils are well-drained Haplorthods of the Rubicon, Blue Lake, or Cheboygan series and are composed of 92.2% sand, 6.5% silt, and 0.6% clay (Nave et al., 2011). The UMBS forest is transitioning from an early successional stage with bigtooth aspen (*Populus grandidentata* Michx.) and paper birch (*Betula papyrifera* Marsh.) dominating the canopy to a mid-successional forest with dominant species of red maple (*A. rubrum* L.), red oak (*Q. rubra* L.), and white pine (*Pinus strobus* L.). The average tree age is roughly 90 years, and mean canopy height is approximately 22 m. Mean peak leaf area index is 3.9 $m^2\ m^{-2}$, and mean stem density of mature trees (diameter at breast height or DBH > 8 cm) is approximately 750 stems per hectare. Red maple stems comprise 6.0 m^2 per hectare with an average DBH of 17.57 ± 5.9 cm. Red oak stems account for 3.7 m^2 per hectare with an average DBH of 25.95 ± 10.3 cm. Trees selected for physiological measurements in this study were representative of this species-size distribution of the forest. Although sap flux analysis measured a variety of sizes and canopy positions, measurements of stem water storage, leaf properties, and xylem water isotopic composition were all made on canopy-dominant individuals in proximity to each other. Additional site details can be found in Gough et al. (2013).

2.2 | Meteorological data

Meteorological measurements were collected at a 46-m eddy covariance tower (Gough & Curtis, 1999). Air temperature, humidity, and atmospheric pressure were recorded every minute and averaged to 10-min block averages (HC-S3, Rotronic Instrument Corp. Hauppauge, NY, USA and PTB101B, Vaisala, Helsinki, Finland). A quantum sensor (LI-190, LI-COR Biosciences, Lincoln, NE, USA) measured incoming photosynthetically active photon flux (PAR). A tipping bucket rain gauge (TE-525, Texas Electronics, Dallas, TX, USA) at the base of the tower measured precipitation. Additional information regarding the instrumentation and analysis approach of the meteorological data at the site is described in Gough et al. (2013) and Maurer, Hardiman, Vogel, and Bohrer (2013).

2.3 | Soil-water potential

Volumetric soil water content and temperature were recorded in four locations at depths of 5, 15, 30, and 60 cm. Two of these locations also included measurements at 100, 200, and 300 cm depths (Hydra probe SDI-12, Stevens Water Monitoring Systems, Inc., Portland, OR, USA; He et al., 2013). Soil moisture is reported as an average across all sensors at the same depth. Following the procedures outlined by He et al. (2013), soil moisture measurements were corrected for systematic bias, estimated for our site as approximately 0.03 $m^3\ m^{-3}$, and smoothed using a 10-hr moving average. Soil water content (θ, $m^3\ m^{-3}$) was vertically integrated over the 3-m soil column. Soil water potential (Ψ_s, MPa) was calculated at each depth from soil moisture data using the Van Genuchten (1980) hydraulic parameterization. Soil hydraulic parameters were derived from pedotransfer functions using the percentages of sand, silt, and clay (92%, 7%, and 1%) for our plots (He et al., 2013).

2.4 | Sap flux

Sap flux was monitored in red maple (n = 8) and in red oak (n = 10) via Granier-style thermal dissipation probes (Granier, 1987; Table 1). Sap flux trees were selected to capture a variety of sizes and canopy positions to enable analysis at the plot-scale for comparison with eddy covariance measurements. Pairs of 20-mm-long probes were inserted into the sapwood at breast height, and the upper probe was continuously supplied with 0.2 W of heating power. Data were recorded every minute and averaged to half-hour intervals. For trees where the sapwood depth was less than the 20-mm sensor length, we applied the Clearwater, Meinzer, Andrade, Goldstein, and Holbrook (1999) correction. Sensor data were processed using a baselining procedure, using periods when the 2-hour average vapor pressure deficit (VPD) was less than 0.5 kPa to allow for nightly recharge flow (Oishi, Oren, & Stoy, 2008). Baselines were determined with respect to the maximum nocturnal temperature for each sensor in order to account for any variation between sensors. Voltage differences between each pair of probes were converted to sap flux density (J_s g H_2O $m^{-2}{}_{sapwood}\ s^{-1}$) following Granier (1985). Sapwood depth at breast height was estimated from species- and plot-specific allometric equations developed by Bovard, Curtis, Vogel, Su, and Schmid (2005) and Matheny et al. (2014b). Sap flux density was converted to sap flow (g s^{-1}) by

TABLE 1 Numbers and size ranges of sample trees used for each group of tree measurements

Sap flux	Red maple	Red oak
Measurement dates: May 1 to September 31, 2014		
Number of individuals	8	10
DBH range (cm)	11.9–22.3	21.7–37.2
Stem water storage Measurement dates: July 10 to September 14, 2014		
Number of individuals	1	1
DBH (cm)	21.3	29.6
Leaf level measurements Measurement dates: June 23 to July 12, 2014		
Number of individuals	3	3
DBH range (cm)	19.2–28.7	24.0–33.5
Xylem cores Measurement dates: June 29, July 9–13, August 4–8, 2014		
Number of individuals	5	5
DBH range (cm)	22.8–37.2	33.5–47.9
Growth measurements Measurement dates: annually from 2001 to 2014		
Number of individuals	423	114
DBH range (cm)	8.2–40.6	9.5–58.5

Note. DBH = diameter at breast height.

multiplying J_s by the sapwood area of the individual tree. Data collected in this experiment were part of a larger study of plot-level sap flux (n = 42 trees of five species). During the 2014 growing season, plot-scaled sap flux comprised 78% of latent heat flux as measured through eddy covariance. Full details of the plot-level sap flux experiment are described in Matheny et al. (2014b).

2.5 | Stem water storage

Stem water storage was continuously monitored in one mature, canopy-dominant individual of each species, red oak and red maple, from July 10 until September 14, 2014 (days of year, DOYs 191–257). Ruggedized soil moisture sensors (model GS-3, Decagon Devices, Pullman, WA, USA) were installed at two different heights: at the base of the trunk (0.5 m above the ground) and just below the live crown (approximately 5.5 m from the ground). Conductive tissue depth was estimated at each sensor location using the measured diameter at that location in place of DBH with the sapwood-DBH allometry provided for the site (Bovard et al., 2005; Matheny et al., 2014b). To avoid heartwood penetration past the red oak's shallow sapwood depth, we trimmed sensor tines to the depth of sapwood for each location. Dielectric potential was recorded by the stem water storage sensors via frequency domain reflectometry every minute and averaged to the half hour. Prior to installation, stem water storage sensors were calibrated to the different densities of oak and maple wood (Matheny et al., 2015). These species-specific calibration equations were then used to convert dielectric potential to volumetric water content (VWC). Stem storage (kg) was calculated for each tree by integrating VWC over the conductive volume of the bole. Full details of sensor calibration, installation, and data processing are provided in Matheny et al. (2015).

2.6 | Leaf-level measurements

Leaf water potential was measured in canopy-top leaves of mature red oak and red maple trees exposed to full sun using a pressure chamber (Model 600 PMS Instrument Co., Corvallis, OR, USA). Leaves were accessed via a mobile canopy lift. Two leaves from each species were tested three times per day from June 23 to July 12, 2014 (DOYs 174–193). Measurements were made at roughly 6:00 (dawn), 13:30 (noon), and 16:00 (afternoon). Directly prior to measurement, the petiole was cut and inserted into the compression gasket, which was then tightened securely around the stem. Internal chamber pressure was increased until moisture was visible on the petiole. The corresponding pressure was denoted as Ψ_L (MPa).

Leaf-level stomatal conductance and photosynthesis were observed *in situ* on the same trees from which leaf water potential was measured. Conductance and photosynthesis were measured using a portable infrared gas analyzer (IRGA; LI-6400, LI-COR Biosciences, Lincoln, NE, USA). One leaf per species was measured daily at 13:30 (noon) and 16:00 (afternoon). Each leaf was measured four times per sampling period with a replication rate of 30 s. Ambient CO_2 inside the chamber was set at 370 ppm, controlled by the LI-6400 CO_2 injection system, and humidity was adjusted with chemical scrubbers to 50%. Leaf temperature was set to 28 °C using the LI-6400 built-in temperature regulator, and ambient radiation was used and recorded. Average leaf temperature during measurement was 27.4 ± 2.5 °C for red maples and 27.1 ± 2.9 °C for red oaks. Mean relative humidity during measurement was 47.2 ± 7.3% and 49.8 ± 7.9% for red maples and red oaks, respectively. Intrinsic water use efficiency (WUE) was calculated from the cuvette data as carbon gain normalized by stomatal conductance.

2.7 | Tree growth measurements

Bole growth information is collected annually via dendrometer bands located at breast height on a random subset of trees of all species (n = 933) including red maple (n = 423) and red oak (n = 114) (Gough, Vogel, Hardiman, & Curtis, 2010). Measured end-of-season diameters are converted to bole areas, A (cm^2), for each year (i) for all years from 2001 to 2014. Annual percent bole growth per tree is calculated using Equation 1. Only trees with a DBH greater than 8 cm at the beginning of the 14-year period were included in this analysis. Mean annual bole growth is calculated as the mean of the annual percent bole growth over all trees of each species.

$$Growth = \left(\frac{A_{i+1} - A_i}{A_i}\right) * 100\%. \quad (1)$$

2.8 | Xylem water isotopes

Tree cores were extracted using an increment borer from multiple mature, canopy-dominant maple and oak individuals in June, July, and August 2014. To avoid damage from repetitive coring to trees instrumented with sap flow or storage sensors, we selected trees of similar species and size within the same plot. We designed our sampling to constrain within- and between-species variability in addition to temporal variability. On June 29, 2014 (DOY 180), we collected

cores from five oaks and four maples to sample within-species variability. To monitor temporal variability, we collected cores from two individuals of each species daily from July 9 to 13 (DOYs 190–194) and August 4 to 8 (DOYs 216–220). Extracted cores were placed in 20 ml scintillation vials with a poly-cone lined cap (Wheaton, Millville, NJ, USA) and kept frozen at −80 °C until analysis.

The isotopic composition of xylem water in the cores was determined using a Picarro L2120-i Cavity Ringdown Spectrometer (CRDS) coupled to a Picarro A0213 Induction Module (IM, together, IM-CRDS). Samples were prepared for the IM by placing a approximately 1-mm-thick slice of xylem into a folded metal strip and loading the xylem-strip assembly into a glass vial purged with zero dry air. Water is extracted by the IM via heating with a programmed induction coil. A carrier stream of zero dry air transports the evaporated water to the analyzer. The CRDS software package (Picarro, Inc., Santa Clara, CA, USA) calculates the isotopic composition of the sample as a mass-weighted integral across the peak. We calibrated measured isotopic compositions to the Vienna Standard Mean Ocean Water (VSMOW) standard (e.g., Coplen, 1996) using lab standards of known isotopic composition. To perform the calibrations, we transferred 4 μL of our internal lab standards onto a piece of glass filter paper and loaded the filter paper into a metal sample holder identical to those used to analyze the cores. We then measured the isotopic composition of water in the filter paper using an identical procedure as used for the tree cores. From these values, we developed a linear transfer function from measured analyzer values to the VSMOW scale. All tree core samples and standards were analyzed a minimum of three times. We express our isotopic compositions in delta notation as part-per-thousand deviations from the VSMOW standard (e.g., $\delta = 1000[(R_{sample}/R_{VSMOW}) - 1]$, where R is the heavy-to-light stable isotope ratio). Median standard errors across all xylem samples were 0.3‰ for $\delta^{18}O$ and 1.1‰ for δD. Deuterium excess (d = $\delta D - 8\delta^{18}O$), which is typically thought to reflect the magnitude of kinetic fractionation, is calculated following the definition by Dansgaard (1964). Lower values of d in xylem water indicate a more evaporated, surficial soil water source and higher values of d indicate water less affected by evaporation, such as deep soil water or groundwater (Simonin et al., 2014).

The IM-CRDS method is faster and less expensive on a per-sample basis than traditional cryogenic distillation techniques (e.g., Ehleringer et al., 2000). However, the technique is new and therefore, the data require careful consideration (e.g., Berkelhammer et al., 2013). We outline below four potential concerns. First, volatile organic compounds in the tree core samples can interfere with spectroscopic isotopic measurements, including CRDS techniques (West, Goldsmith, Matimati, & Dawson, 2011). This bias results from spectroscopic overlap of wavelengths absorbed by both water and organic molecules. The IM seeks to minimize this potential bias by removing organic molecules through (a) adsorption to a heated activated carbon column and (b) oxidation by a micropyrolysis column maintained at 1200 °C (e.g., Berkelhammer et al., 2013). Second, isotopic values in CRDS measurements depend weakly on water vapor concentration, and the correction varies by instrument and can vary through time (Tremoy et al., 2011). To minimize the potential influence of this bias, we optimized the IM heating recipe to our samples such that (a) water vapor concentrations were kept as constant as possible through the peak and (b) peak shapes were similar across maple, oak, and standard samples. Third, isotopic memory effects can influence measured compositions (e.g., Berkelhammer et al., 2013; Gupta et al., 2009). Instrumental memory occurs when residual vapor from prior analyses remains in the analyzer cavity and is measured during subsequent analyses. The influence of memory on the measured isotopic value depends on the magnitude of isotopic difference between subsequent samples. We monitored for instrumental memory effects by looking for a linear trend in the isotope values from the first few analyses of a sample, and we discarded the values where strong memory effects were apparent. We observed the strongest memory effects between samples of the lab standards used, which were more isotopically distinct from each other than the maple and oak samples were from each other. Therefore, we expect the implications of instrumental memory to be small. Finally, water extraction by IM-CRDS is sensitive to the rate and duration of sample heating. Ideally, the induction coil should heat the sample just until all of the water is removed. The sample may combust with further heating, leading to water isotope values that are biased by combustion-derived water. We monitored our analyses for combustion through visual inspection of the core sample for charring and of the analyzer peaks following analysis. Combustion water introduces a long tail to the water concentration peak and marked deviations in measured isotope values. Analyses that were influenced by combustion were omitted. While we strived to minimize instrumental bias from known sources, we note that the IM-CRDS procedure has yet to undergo extensive validation. Regardless, we maintain that our xylem water measurements record environmental water sources and variability as xylem water compositions closely match local environmental waters, and measurements across all samples were consistent.

2.9 | Analysis of liquid water samples

We collected samples of local precipitation and nearby surface and ground waters to constrain the isotopic composition of likely tree water sources. Surface and ground water samples were collected in 20-ml scintillation vials and were sealed with a poly-cone lined cap until isotopic analysis. We collected surface water from Douglas Lake on UMBS property and a stream approximately 1 km southwest of Douglas Lake. Four precipitation samples were collected approximately biweekly from mid-June until mid-August in a bucket with a layer of mineral oil to prevent evaporation (Scholl, Ingebritsen, Janik, & Kauahikaua, 1996; Friedman, Harris, Smith, & Johnson, 2002). We collected precipitation from the bucket by using a syringe to extract precipitation from below the layer of mineral oil. After collection, the bucket was emptied, cleaned, dried, and a layer of mineral oil replaced for the next sample.

We analyzed the isotopic composition of the liquid samples with a Picarro L2120-i CRDS coupled to an A0211 high-precision vaporizer and attached autosampler. We monitored for organic contamination using the Picarro ChemCorrect software (e.g., West et al., 2011). Standard errors for liquid water $\delta^{18}O$ and δD were below 0.1‰ and 0.4‰, respectively.

2.10 | Sensitivity analysis

We conducted a sensitivity analysis using the Finite-difference Ecosystem-scale Tree Crown Hydrodynamics model version 2 (FETCH2; Mirfenderesgi et al., 2016). The FETCH2 model approximates water flow through a tree's xylem system as flow through unsaturated porous media (Sperry, Adler, Campbell, & Comstock, 1998) with conductance and capacitance changing dynamically in response to stem water potentials. A full model description and formulation are provided in Mirfenderesgi et al. (2016) and Bohrer et al. (2005). We tested all eight combinations of each studied opposing trait pair along the three axes of hydraulic control (Figure 1): (a) deep roots, anisohydric stomatal regulation, and ring-porous wood; (b) deep roots, anisohydric stomatal regulation, and diffuse-porous wood; (c) deep roots, isohydric stomatal regulation, ring-porous wood; (d) deep roots, isohydric stomatal regulation, and diffuse-porous wood; (e) shallow roots, anisohydric stomatal regulation, and ring-porous wood; (f) shallow roots, anisohydric stomatal regulation, and diffuse-porous wood; (g) shallow roots, isohydric stomatal regulation, and ring-porous wood; and (h) shallow roots, isohydric stomatal regulation, and diffuse-porous wood.

The FETCH2 model incorporates plant traits at the leaf, stem, and root levels through suites of parameters affecting water transport at each level. Two leaf trait parameters, C_3 and Φ_σ, define stomatal response to leaf water potential and can be tuned to represent isohydry and anisohydry. Φ_σ is the inflection point in the stomatal response to xylem water potential (MPa), C_3 is a unitless shape parameter for stomatal response to xylem water potential, and n represents the model's time step. We approximated values for these parameters based on leaf water potential data for red oaks and red maples in our site reported in the present study and by Thomsen et al. (2013) (Table 2 and Figure 2).

$$\beta = \frac{E^{(n)}{}_{\mathrm{v}}}{E^{(n)}{}_{\mathrm{v,max}}} = \exp\left[-\left(\frac{\Phi^{(n-1)}}{\Phi_\sigma}\right)^{C_3}\right], \tag{2}$$

where β is the response of stomatal conductance to changes in xylem water potential, $E^{(n)}{}_v$ is the FETCH2 calculated actual transpiration (g s^{-1}), $E^{(n)}{}_{\mathrm{v,max}}$ is the half-hourly potential evaporative demand determined from canopy-top atmospheric conditions used to force the model (g s^{-1}), and Φ is the xylem water potential calculated by the FETCH2 model (MPa).

Parameters that describe stem level traits, Φ_{50} and $\Phi_{88,}$ represent the xylem water potentials (MPa) at 50% and 88% relative water content (RWC), respectively, and are used to describe the capacitance in response to changing xylem water potentials. Due to the paucity of measurements of RWC alongside stem water potential in the literature, values for Φ_{50} and Φ_{88} were approximated on the basis of observed reliance on stem water storage in this study and the values obtained through model optimization by Mirfenderesgi et al. (2016) for oak species (Table 2 and Figure 2).

$$\mathrm{RWC} = 1 + \frac{\Phi}{(b\Phi - \Phi_{50}(2+b))}, \tag{3}$$

where b is calculated as follows:

$$b = \frac{\Phi_{88} - 0.24\Phi_{50}}{0.12(\Phi_{50} - \Phi_{88})}. \tag{4}$$

$K_{\max}$ (kg m^{-1} s^{-1} MPa), C_1 (MPa), and C_2 represent the maximum xylem conductance and the shape of the xylem vulnerability curve, respectively, and are used to calculate dynamic changes in actual xylem conductance, $K_{\max}$ (kg m^{-1} s^{-1} MPa). Together, these stem-level traits represent the effects of xylem architecture on transpiration. Values used for $K_{\max}$ were reported by Maherali, Moura, Caldeira, Willson, and Jackson (2006) for red oak and red maple in Duke Forest in Durham, NC (Table 2).

$$K = A_{\mathrm{sapwood}}\, K_{\max} \exp\left[-\left(\frac{-\Phi}{C_1}\right)^{C_2}\right], \tag{5}$$

where A_{sapwood} refers to the sapwood area of the tree (m^2). C_1 and C_2 were calculated from reconstructed xylem vulnerability curves for red oak and red maple using the observed values for 50% and 88% conductivity loss provided in the database xylem water potentials compiled in Choat et al. (2012, Supplemental material) (Table 2 and Figure 2). For this analysis, all structural properties of the simulated tree (e.g., sapwood area, crown area, leaf area index, vertical distribution of leaves, tree height, DBH, and stem taper) were held constant to allow for isolated, direct comparisons of the effects of differing hydraulic parameter sets.

Because FETCH2 lacks an explicit representation of the root component, we prescribed water potentials to serve as the model's boundary condition for the top of the root system and base of the stem. We represented deep roots by prescribing a constant high water potential, −0.033 MPa, typically referred to as field capacity (Rawls, Brakensiek, & Saxton, 1982). A shallow rooting strategy was simulated by water potential that steadily declined over the 7-day

TABLE 2 Trait values and references for parameters used to test FETCH2 sensitivity to leaf and stem level traits

Organ	Trait	Risk prone	Risk adverse	Reference
Leaf	C_3	4 (unitless)	7 (unitless)	Approx. from Thomsen et al. (2013)
	Φ_σ	−2.5 MPa	−1.2 MPa	Approx. from Thomsen et al. (2013)
Stem	ϕ_{50}	−2.5 MPa	−2.0 MPa	(Mirfenderesgi et al., 2016)
	ϕ_{88}	−0.5 MPa	−0.3 MPa	(Mirfenderesgi et al., 2016)
	$K_{\max}$	1.33 kg m^{-1} s^{-1} MPa	0.55 kg m^{-1} s^{-1} MPa	(Maherali et al., 2006)
	C_1	−1.99 MPa	−2.58 MPa	Calc. from Choat et al. (2012)
	C_2	1.71 (unitless)	1.35 (unitless)	Calc. from Choat et al. (2012)

Note. FETCH2 = Finite-difference Ecosystem-scale Tree Crown Hydrodynamics model version 2.

Note. Risk-prone strategies indicate anisohydry or ring-porous xylem.

Note. Risk-adverse strategies represent isohydry or diffuse-porous xylem.

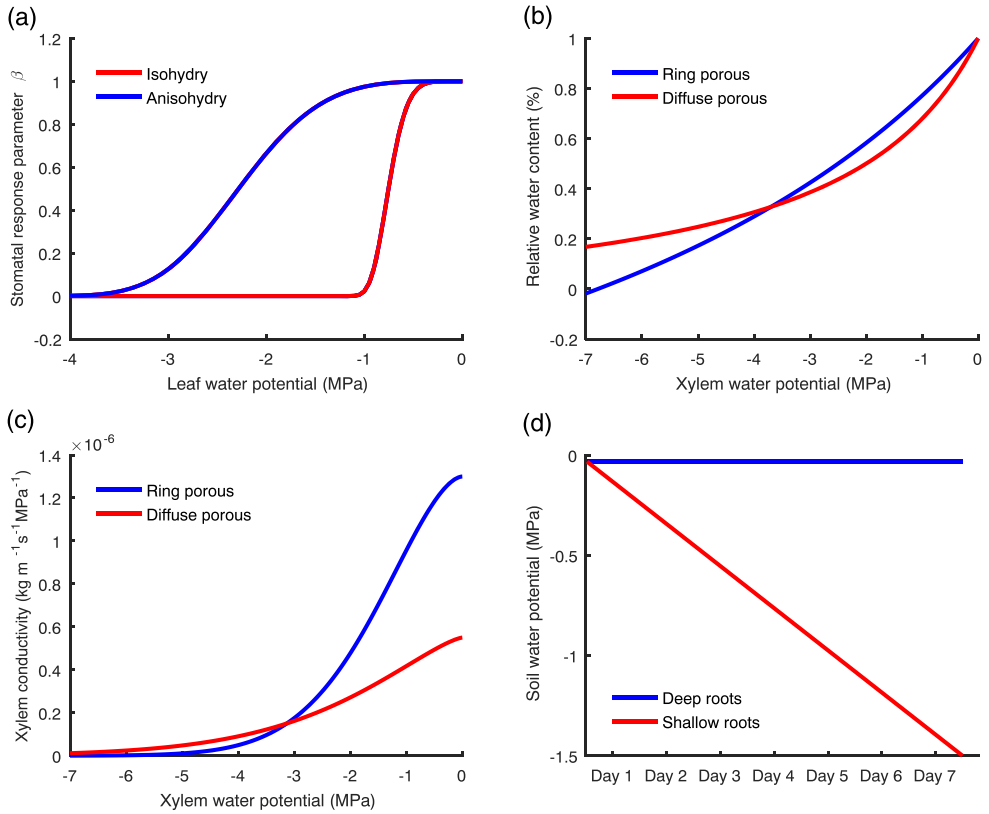

FIGURE 2 Characterization of the different hydraulic traits: (a) Isohydric and anisohydric responses of stomatal conductance (β) as a function of leaf water potential. Weibull-shaped response curves are defined by C_3 and Φ_σ as given for anisohydry (risk prone) and isohydry (risk adverse) in Table 2. (b) Response of relative xylem water content to stem water potential as approximated for ring-porous (left) and diffuse-porous (right) trees. Curve shapes are defined by Φ_{50} and Φ_{88} for ring-porous (risk prone) and diffuse-porous (risk adverse) as listed in Table 2. (c) Xylem conductivity for ring- and diffuse-porous species as constructed using values for red oak and red maple from Choat et al. (2012). Curve shapes are defined by parameters C_1 and C_2 as listed for ring-porous (risk prone) and diffuse-porous (risk adverse) species in Table 2. (d) Water potential at the top of the root system (bottom-of-stem boundary condition) during a week-long dry-down event, as prescribed for cases having deep and shallow roots

dry-down simulation period from −0.033 MPa (field capacity) to −1.5 MPa, the permanent wilt point (Rawls et al., 1982) (Figure 2). We forced the model using potential transpiration calculated from the above canopy conditions as measured at our field site on July 17, 2013, a sunny day with minimal cloud cover and low-to-moderate VPD (maximum half-hourly PAR = 1,817.5 μmol m^{-2} s^{-1}, mean temperature = 27.6 °C, and maximum half-hourly VPD = 2.6 kPa). We recycled these conditions for seven simulation days. Potential transpiration was determined following Mirfenderesgi et al. (2016, Appendix A).

3 | RESULTS

During the peak growing season of 2014, between July 10 (DOY 191) and September 30 (DOY 273), daily peak sap flux averaged 40.8 ± 14.3 g m^{-2} s^{-1} for red maples and 39.8 ± 12.4 g m^{-2} s^{-1} for red oaks. During this period, stem-stored water use averaged 4.8 ± 2.9 kg day^{-1} in red maple and 2.9 ± 2.4 kg day^{-1} in red oak. Withdrawal from storage, or the diurnal fluctuation in the amount of stem-stored water, was largest in red maples when soil water was non-limiting and tended to be between 5 and 10 kg day^{-1}. Intrinsic WUE for red maple (101.1 μmol CO_2 mol^{-1} H_2O) exceeded that of red oak (84.1 μmol CO_2 mol^{-1} H_2O) by 16.9%.

Soil water content decreased by 20% from DOYs 211 to 223 (July 30 to August 11), constituting a 2-week "mini-drought" (Figure 3a). Red maple sap flux and stem water storage were strongly affected by this decrease in soil water content, but red oak water fluxes were not. During this period of limited soil moisture, mean daily maximal sap flux in red maples fell from 59.8 ± 30.6 g m^{-2} s^{-1} (at DOY 211) to 11.5 ± 6.4 g m^{-2} s^{-1} (at DOY 223), a reduction of over 80%. For the same time period, maximum daily sap flux from red oaks declined by only 31%, from 46.7 ± 14.9 to 32.4 ± 10.6 g m^{-2} s^{-1} (Figure 3b). Concurrently, maximum daily stem water storage in red maple fell by 28% from 100.0 to 72.1 kg, but remaining nearly constant (between 108.3 and 107.2 kg, i.e., <1% decrease) in red oak (Figure 3c). During the mini-drought, diurnal withdrawal from storage by red maple fell from 13.4 kg on DOY 213 to 0.78 kg on DOY 222. Red oaks demonstrated an opposing pattern. Daily storage withdrawal in red oaks ranged from 0 to 5 kg when soil water was non-limiting, but rose from 4.0 kg on DOY 211 to 8.4 kg on DOY 222.

To isolate the effect of soil water content on sap flux, we first conducted a multiple linear regression between integrated daily sap flux, total daily PAR, and daily maximum VPD (R^2 = .268 and .274 for red maple and red oak, respectively, and P < .0001 for both). We used the residual sap flux from this regression model to calculate a second linear regression against Ψ_s at every measurement depth between 5 and 300 cm (n = 7) (Table 3). Due to the non-linear nature of Ψ_s, we

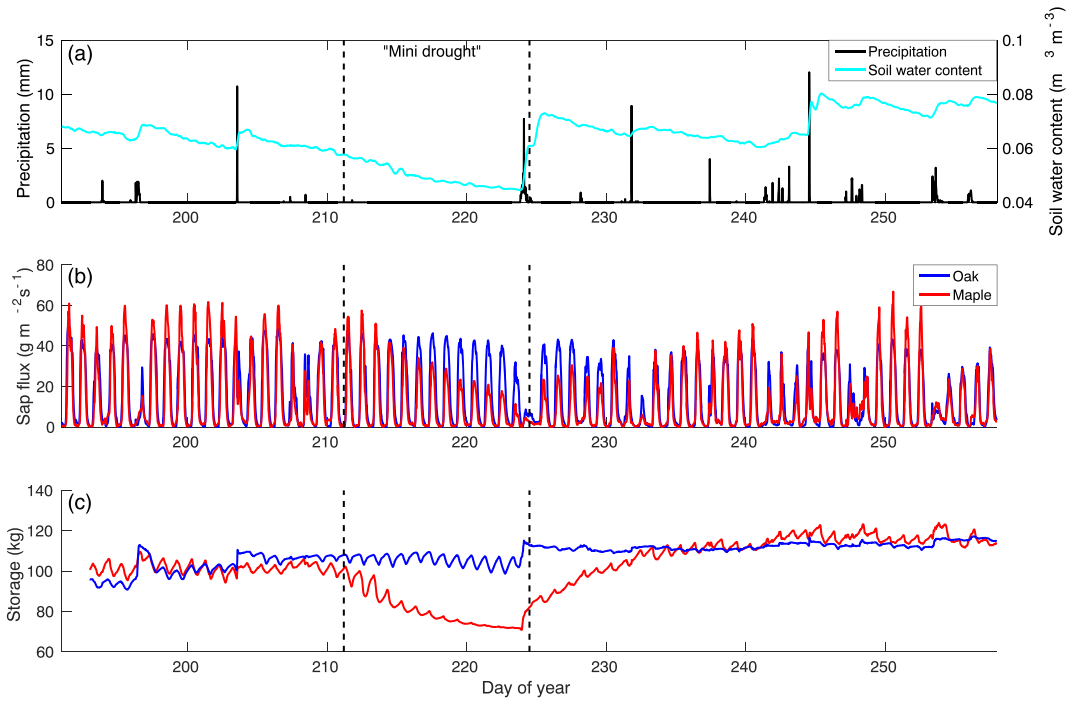

FIGURE 3 (a) Precipitation (mm) and soil water content ($m^3\ m^{-3}$) integrated across the 3-m soil column, (b) Mean sap flux ($g\ m^{-2}\ s^{-1}$) for red oak (n = 10) and red maple (n = 8) trees, and (c) Stem water storage (kg) for day of year 191–260, 2014. The 2-week period of an inter-storm dry-down, or "mini-drought" (DOYs 211–224), is marked by dashed vertical lines. DOY, day of year

TABLE 3 Seasonal mean soil moisture (θ, $m^3\ m^{-3}$) and standard deviations for each measurement depth. Linear regression statistics for the relationship between residual sap flux and all seven soil moisture measurement depths between 5 and 300 cm. Residual sap flux is the residual generated by a linear regression of sap flux (dependent variable) and PAR, VPD, and Ψ_s (independent variables)

Depths	Mean seasonal θ $m^3\ m^{-3}$	Red maple		Red oak	
		P values	R^2	*P* values	R^2
5 cm	0.086 ± 0.024	.1812	.0202	.7638	.0010
15 cm	0.109 ± 0.027	.0001*	.1614	.4075	.0078
30 cm	0.101 ± 0.021	8.9E-6**	.2019	.3045	.0120
60 cm	0.083 ± 0.018	.0003*	.1360	.2756	.0135
100 cm	0.076 ± 0.018	.0002*	.1507	.3231	.0111
200 cm	0.043 ± 0.002	.1590	.0224	.9534	.0000
300 cm	0.044 ± 0.004	.0009*	.1190	.0272**	.0542

Note. PAR = photosynthetically active photon flux; VPD = vapor pressure deficit.

Note. Significant values are indicated with an asterisk, and the most significant relationship for each species is indicated by a double asterisk.

used an inverse log function of the absolute value of Ψ_s to linearize the data following Thomsen et al. (2013). Residual sap flux from red maples demonstrated significant relationships with Ψ_s at every depth except 5 and 200 cm, with the most strongly correlated relationship occurring at 30 cm (P < .0001, R^2 = .20; Table 3). Residual sap flux from red oaks was weakly (though significantly) related to Ψ_s and only at 300 cm (P = .0272, R^2 = .05) (Table 3). Soil moisture between 5 and 100 cm is strongly auto-correlated (mean R^2 = .75, P < .0001). Soil moisture at 200 cm is well correlated with that at 300 cm (R^2 = .57, P < .0001) but is less well correlated with that in the overlying layers (mean R^2 = .26, P < .0001). It is possible that red maples draw upon water throughout the shallow soil column, but the autocorrelation between soil moisture in the shallow layers prevents us from pinpointing precisely where maple root water uptake occurs. However, these results do suggest that oak water uptake occurs at a deeper location than maple water uptake.

Leaf water potential measurements illustrated that each species used different leaf hydraulic strategies. Red maples possessed a narrow range of Ψ_L between −0.12 and −1.2 MPa over the 20-day measurement period. Red oaks showed a larger range, −0.13 to −2.2 MPa, almost double that of maples during the same period. Red maple Ψ_L was not strongly affected by VPD (Figure 4); the only significant relationship between Ψ_L and VPD (P = .0335, R^2 = .21) occurred in the late afternoon (16:00, Figure 4c). Conversely, red oaks demonstrated strong correlations between VPD and Ψ_L during noontime (13:00, Figure 4d; P = .0040, R^2 = .46) and late afternoon (16:00; P = .0117, R^2 = .3195, Figure 4f). Predawn Ψ_L was not correlated with VPD for either species (P > .1).

Oak xylem water exhibited more consistent isotopic compositions than maple xylem water (Figure 5a,b). Maple xylem delta values varied substantially from month to month, but oak xylem isotope compositions did not. For June, July, and August, mean maple compositions were −8.8 ± 0.2‰, −7.2 ± 0.2‰, and −9.6 ± 0.1‰ for $\delta^{18}O$, respectively, and −76.3 ± 0.8‰, −65.0 ± 0.4‰, and −78.9 ± 0.3‰ for δD. In contrast, mean oak xylem compositions for the same time period were −10.6 ± 0.2‰, −10.7 ± 0.2‰, and −10.5 ± 0.1‰ for $\delta^{18}O$ and −81.7 ± 0.6‰, −81.4 ± 1.0‰, and −78.4 ± 0.4‰ for δD. We did not observe any isotopic trends on a day-to-day basis during July and August when cores were collected over multiple days.

Environmental water source compositions bracket the observed xylem water compositions. Precipitation compositions were the most

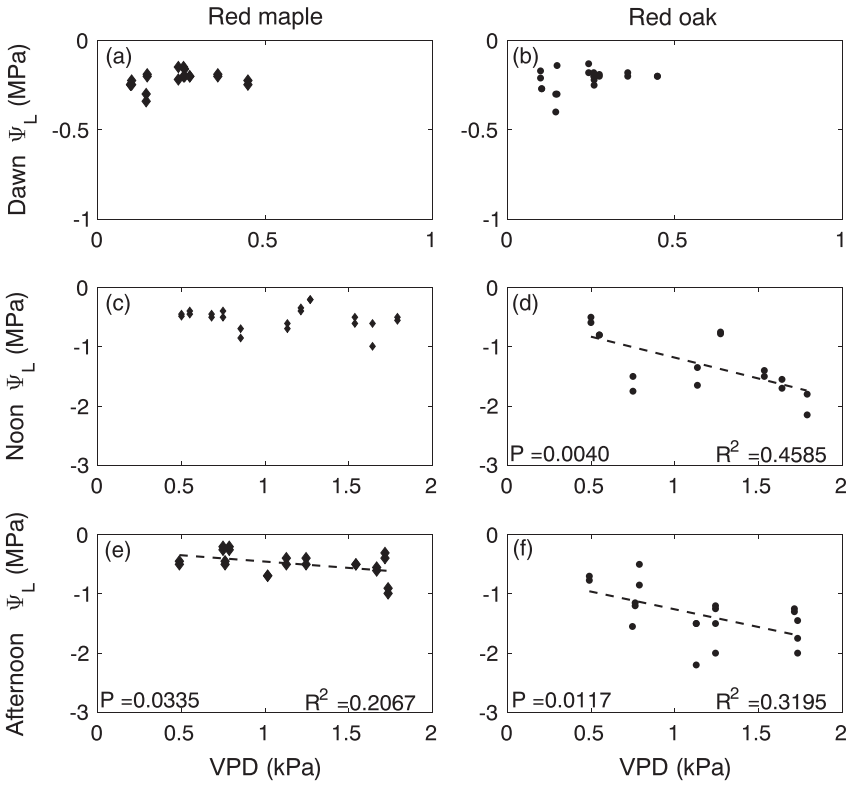

FIGURE 4 Relationships between leaf water potential (Ψ_L, MPa) and vapor pressure deficit (VPD, kPa) at three times during the day for each species. Red oak leaf water potential was correlated with VPD at noon (13:30; panel d, P = .0040, R^2 = .46) and in the afternoon (16:00; panel f, P = .0117, R^2 = .32). Leaf water potential of red maple was weakly correlated to VPD in the afternoon (16:00; panel e, P = .0335, R^2 = .21), but uncorrelated at dawn and noon

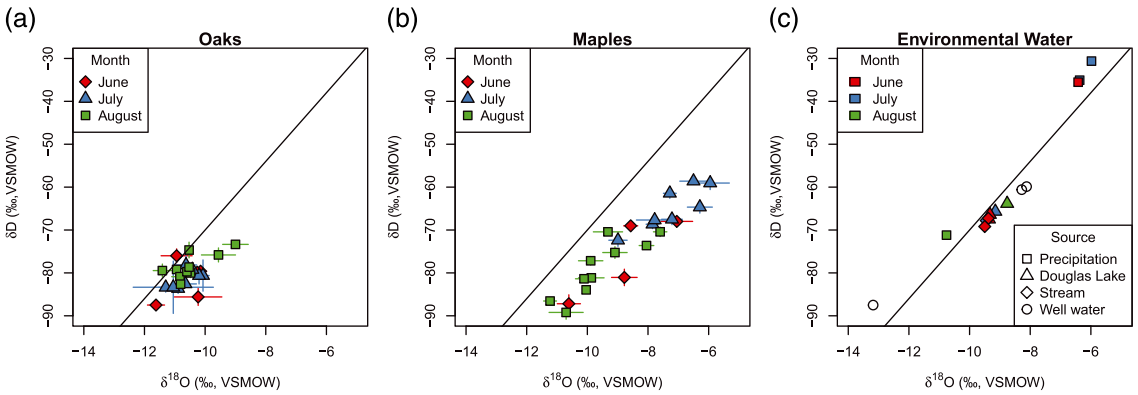

FIGURE 5 (a) Isotopic compositions (δD vs. $\delta^{18}O$) of xylem from red oak samples. (b) Isotopic compositions (δD vs. $\delta^{18}O$) of xylem from red maple samples. (c) Isotopic compositions (δD vs. $\delta^{18}O$) of environmental water samples. Isotopic compositions are reported as per mil deviations from the Vienna Standard Mean Ocean Water (VSMOW) standard. Error bars denote one standard error. Well waters were collected in August only. Samples that were collected in multiple months are color-coded by month. In all panels, the solid black line is the global meteoric water line, which describes the global relationship between δD and $\delta^{18}O$ in precipitation (Craig, 1961). Maple xylem compositions (b) vary more than oak xylem (a) compositions throughout the collection period, indicating that the water sources used by maples are more isotopically variable than those used by oaks

variable, ranging from −5.98‰ to −10.76‰ in $\delta^{18}O$ and −30.62‰ to −71.19‰ in δD from June to August. In contrast, surface water samples collected from Douglas Lake and from the nearby stream were isotopically invariant. Douglas Lake water samples ranged from −9.35‰ to −9.15‰ in $\delta^{18}O$ and −67.49‰ to −65.68‰ in δD, and samples from the stream ranged from −9.38‰ to −9.50‰ in $\delta^{18}O$ and −67.28‰ to −69.19‰ in δD. Finally, we measured the isotopic composition of deeper ground waters from three wells located at the UMBS site. The shallower wells (25 and 47 m depth) had isotopic compositions of −8.12‰ and −8.28‰ for $\delta^{18}O$ and −59.88‰ and −60.59‰ for δD, and the deeper well (130 m depth) had an isotopic composition of −13.18‰ for $\delta^{18}O$ and −87.5‰ for δD. All xylem water samples had lower deuterium excess values than any of the observed precipitation values, with red maple xylem water having substantially lower deuterium excess than that of red oaks (Figure 6).

We analyzed incremental bole growth records from 2001 to 2014 for both species with respect to mean annual soil moisture at 30 cm and total annual precipitation. Because instrumentation at additional soil depths (60 cm and beyond) was not installed until 2010, we were limited in this analysis to soil moisture at 30 cm depth. For both species, mean annual bole growth was uncorrelated with total annual and total growing season rainfall (all P > .1). Mean annual soil moisture at 30 cm was not correlated with total annual rainfall (P > .1). Bole growth was not correlated with mean growing season soil moisture.

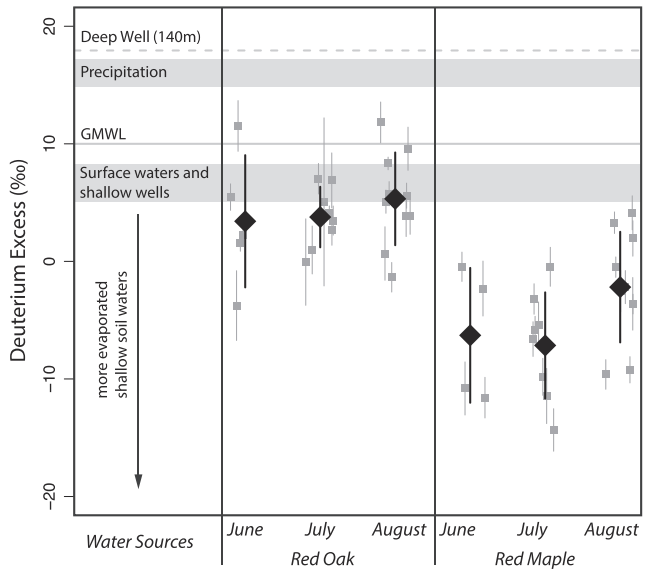

FIGURE 6 Deuterium excess for environmental and xylem water samples.The isotopic ranges observed in environmental water sources that were measured throughout the summer are shown as gray bars. Increasingly negative deuterium excess indicates that more evaporation has occurred. Samples having more evaporated isotopic signatures are associated with shallower water sources. Monthly means are presented by large black diamonds. Error bars on individual points are standard error (grey) and are the standard deviation of the distribution (black). GMWL, global meteoric water line

Bole growth of red maples was positively correlated with mean annual soil moisture (P = .0243, R^2 = .36), but red oak growth was uncorrelated with mean annual soil moisture (P = .08; Figure 7). Among a subsample of trees with the highest growth rates (8 cm < DBH < 20 cm), this relationship was still stronger in maples (P = .0176, R^2 = .40 for red maples and P = .31 for red oaks). For the 5 years of deep soil moisture measurement data (2010–2014), red maple bole growth was correlated with mean annual soil between 15 and 300 cm with an average R^2 of .26. During this period, bole growth for red oak was uncorrelated with mean annual soil moisture at all depths (all R^2 < .09).

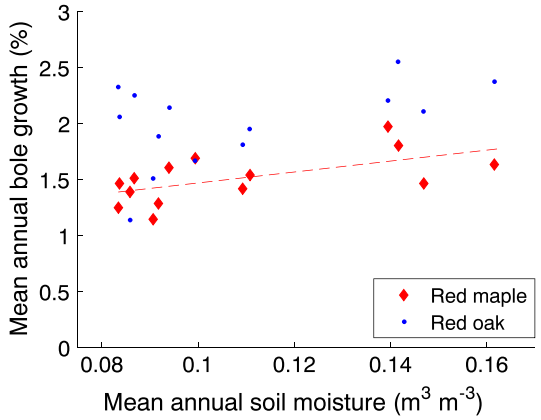

FIGURE 7 Mean annual bole growth (%) for years 2001–2014 for red oak (dots) and red maple (diamonds) as a function of soil moisture at 30 cm depth (m^3 m^{-3}). Bole growth of red maple was strongly correlated with mean annual soil moisture (P = .0243, R^2 = .36), whereas bole growth in red oak was not correlated to mean annual soil moisture (P = .08)

A sensitivity analysis was performed using FETCH2 to test the influence of suites of plant traits at the leaf, stem, and root levels on diurnal transpiration patterns. We used observed plant trait values for red oaks and red maple when they were available (Maherali et al., 2006; Choat et al., 2012; Thomsen et al., 2013), though we aim to compare the influence of traits at each level and the potential interactions between them rather than to replicate the exact behavior of our studied trees. In the test case for "deep roots," the combinations of anisohydry and ring-porous xylem (simulation case 1, roughly representative of the trait combination in red oak) allowed the highest transpiration rates relative to other trait combinations. Anisohydry paired with diffuse-porous xylem (simulation case 2) and isohydry paired with ring-porous xylem (simulation case 3) yield similar predicted transpiration, but the isohydry/diffuse-porous xylem combination (simulation case 4) exhibits the lowest predicted transpiration (Figure 8).

For simulations using drying soil conditions, considered representative of a shallow rooting strategy during an inter-storm dry-down period (simulation cases 5–8) (Figure 8), the trait combinations representing anisohydry paired with ring-porous wood (simulation case 5) produced the largest simulated transpiration. Transpiration from isohydric/ring-porous (simulation case 7) and anisohydric/diffuse-porous (simulation case 6) combinations began at relatively similar levels when soil water was abundant (Figure 8), but the two trait pairs diverge as soil moisture declines, with the isohydric/ring-porous combination curtailing transpiration more quickly than the anisohydric/diffuse-porous combination (Figure 8). Transpiration predicted for the isohydric diffuse-porous (simulation case 8, roughly representative of the trait combination in red maple) species remained the lowest of the four tested combinations. The isohydric/ring-porous simulation (simulation cases 3 and 7) displayed relatively flat transpiration throughout the course of the day regardless of soil (root) water access, typical of the isohydric stomatal strategy. The three remaining leaf and xylem trait combinations (anisohydry/ring-porous, isohydry/diffuse-porous, and anisohydry/diffuse-porous) for both deep and shallow root cases (Figure 8) all demonstrate a diurnal water flux skewed towards the morning hours, with the anisohydry/diffuse-porous case (simulation cases 2 and 6) as the most extreme.

4 | DISCUSSION

4.1 | Stem strategy

Although red oaks and red maples perform comparably under well-watered conditions, differences in hydraulic strategies and controls lead to disparate trends in water flux when soil moisture is low. During periods of adequate soil moisture, sap flux was greater in red maples than in red oaks (Figure 3). Similar trends were shown for these species in our site in a previous study conducted by Bovard et al. (2005), as well as for different species of oak and maple at other sites (Oren & Pataki, 2001; von Allmen et al., 2014). However, when soil moisture was limiting, sap flux and stem water storage declined substantially in red maples but not in red oaks. In a concurrent study, stem water storage and daily storage withdrawal in red maples were significantly correlated with Ψ_s (Matheny et al., 2015). Likewise, after controlling

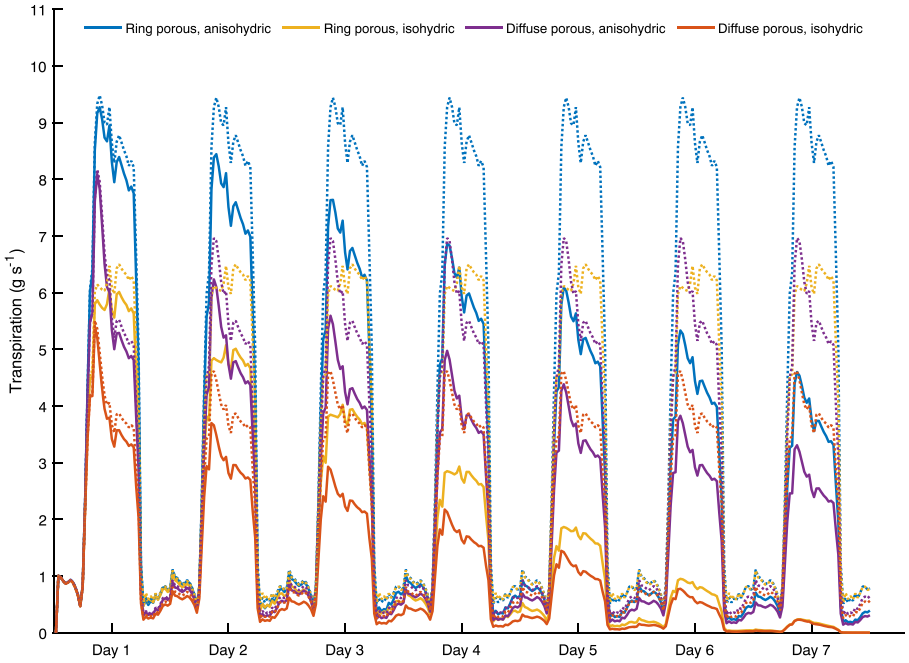

FIGURE 8 Sensitivity of simulated FETCH2 transpiration to different combinations of emergent leaf trait (isohydry or anisohydry) and xylem structure (ring- or diffuse-porous) assuming steady access to high (less negative) soil water potential afforded through a deep rooting strategy (dotted lines) or a shallow rooting strategy (solid lines). The shallow rooting strategy is described by steadily declining soil water potential (from −0.033 MPa on day 1 to −1.5 MPa on day 7). FETCH2, Finite-difference Ecosystem-scale Tree Crown Hydrodynamics model version 2

for the effects of PAR and VPD, residual sap flux in red maples was significantly correlated with Ψ_s at multiple shallow depths, but residual sap flux in red oaks was correlated with Ψ_s at only 300 cm (Table 3). In oaks, sap flux and stem water storage were only moderately impacted by the mini-drought, although both declined by large degrees in maples (Figure 3). Matheny et al. (2015) found that stem water storage in oaks was only significantly positively correlated with Ψ_s when soil was wettest and that a negative correlation existed between withdrawal from storage and Ψ_s, indicating that oaks relied upon stem-stored water for transpiration during times of depleted soil water only. Conversely, red maples were found to rely heavily on daily withdrawal from storage to supply the diurnal transpiration stream (Matheny et al., 2015). The limited reliance on diurnal storage withdrawal by red oak and the larger reliance on stored water by red maple are consistent with observations made in other ring- and diffuse-porous species (Wullschleger, Hanson, & Todd, 1996; Kocher, Horna, & Leuschner, 2013). Meinzer et al. (2013) similarly revealed that in a mixed deciduous forest in Pennsylvania, diffuse-porous species were twice as sensitive to changes in soil moisture as co-occurring ring-porous trees.

4.2 | Leaf strategy

In addition to their xylem architecture differences, red oaks and red maples exhibit distinct patterns of stomatal regulation. Although isohydry and anisohydry are typically discussed with respect to Ψ_s, we aim to create a discussion of whole-plant hydraulics where water status in each organ is linked, in order, along the soil-root-stem-leaf-atmosphere continuum. Therefore, we chose to relate Ψ_L to the atmospheric VPD during each measurement period (following stomatal optimization theory), rather than directly to soil moisture (following cohesion-tension theory; Novick, Miniat, & Vose, 2015). The strong noon and afternoon correlations between Ψ_L and VPD in red oak are characteristic of an anisohydric hydraulic strategy, where transpiration is sustained at highly negative Ψ_L (Figure 4d,f). In contrast, the weak relationship between Ψ_L and VPD during the afternoon in red maple represents a more isohydric strategy (Figure 4e). These results agree with the traditional method of comparing Ψ_L to Ψ_s (Thomsen et al., 2013). In a synthesis analysis, 12 out of the 13 *Quercus* species studied exhibited anisohydric stomatal regulation, despite the increased embolism vulnerability associated with ring-porous xylem (Martinez-Vilalta et al., 2014). Maherali et al. (2006) demonstrated that species with more vulnerable xylem architectures, including seven species of *Quercus*, tended to have higher stomatal conductance and photosynthetic rates. Under all soil water conditions, leaf WUE was greater in red maples than in red oaks. Similarly, higher WUE has been documented in isohydric genotypes of poplars than their anisohydric counterparts (Attia, Domec, Oren, Way, & Moshelion, 2015). Higher WUE is expected for isohydric species that limit stomata opening to times when VPD is low, causing less water loss from the stomata per unit CO_2 assimilated.

4.3 | Root strategy

Several studies postulate that a deep rooting strategy allows oaks to maintain transpiration at low Ψ_L in spite of their risk-prone vasculature and anisohydric stomatal regulation strategies (e.g., von Allmen et al., 2014; Bovard et al., 2005; Oren & Pataki, 2001; Matheny et al., 2014b; Thomsen et al., 2013; Abrams, 1990; Baldocchi & Xu, 2007; Hernandez-Santana et al., 2008). However, few offer clear evidence of water uptake from deep roots (Miller et al., 2010; Phillips &

Ehleringer, 1995). Our xylem water isotope measurements indicate differential water uptake between the two species with oaks preferentially taking up more water from deeper roots than maples. The more consistent isotopic compositions observed in red oak xylem water relative to that in red maple imply that oaks obtain water from a more consistent water source than maples (Figure 5). The isotopic variability of soil water decreases with depth in the soil column (e.g., Barnes & Turner, 1998; Breecker, Sharp, & McFadden, 2009). Near the surface, the isotopic composition of soil water reflects a balance between precipitation and evaporation and can change substantially after individual precipitation events (e.g., Gazis & Feng, 2004; Barnes & Allison, 1988). For our site, the standard deviation around the mean seasonal soil moisture declines dramatically below 100 cm (Table 3). We interpret this depth to be near the threshold of extent for large evaporation effects on soil moisture. During dry inter-storm periods, evaporation from the soil surface enriches the residual water in heavy isotopes. As a result, soil water above approximately 100 cm shows strong isotopic change on timescales of days to weeks. In contrast, isotopic compositions of deeper soil water (> approximately 100 cm) exhibit less variability because they are not subject to the direct effects of evaporation, and water infiltrates to these depths only during large precipitation events (Barnes & Turner, 1998). Xylem water isotopes of red maple were observed to vary strongly throughout the season, and track towards precipitation compositions (Figure 5 and Figure 6). This suggests that red maples predominantly use shallow water sources, consistent with the high correlations observed between sap flux and Ψ_s from approximately 15 to 100 cm (Table 3). In contrast, red oak xylem water compositions are more constant throughout the growing season, implying a deeper, less variable water source (Figure 5 and Figure 6). This is consistent with the observation that sap flux is only significantly correlated with the deepest Ψ_s measured (300 cm, Table 3).

The relationship between the $\delta^{18}O$ and δD compositions in extracted xylem water provides additional isotopic evidence for water source differentiation. Evaporation from the top soil layers fractionates $H_2{}^{18}O$ relative to $H_2{}^{16}O$ more than $HD^{16}O$ relative to $H_2{}^{16}O$ as a result of the larger mass difference between the former pair of isotopologues compared to the latter. Therefore, evaporated water will deviate strongly from the meteoric water line and have lower deuterium-excess values (d-excess, $d = \delta D - 8\delta^{18}O$). Several studies have shown that rooting depth can be inferred from the d-excess parameter, with lower d-excess values implying a shallower rooting depth (West et al., 2012; Simonin et al., 2014, Dawson & Simonin, 2011; Dawson, 1993). Deuterium-excess values for red maple are generally lower than red oak (Figure 6). These values were also lower than any of the environmental water sources sampled, likely due to evaporation between soil infiltration and root uptake. In contrast, oak xylem water d-excess values overlap with the values observed for local surface waters and for shallow ground water sampled from wells (Figure 6). These results demonstrate that red maple predominantly uses shallow soil waters, but red oak uses deeper soil waters.

4.4 | Whole-plant hydraulic strategy

The proposed safety–efficiency trade-off is typically discussed with respect to traits existing within the same plant organ (i.e., xylem; Manzoni et al., 2013; Gleason et al., 2016). However, if we extend the theoretical concept to the emergent whole-plant hydraulic framework, we could consider red oaks and red maples within our research site as representations of opposing ends of this spectrum. Red oaks did not exhibit the water stress that would be predicted from their cavitation risk-prone xylem architecture and leaf hydraulic strategy. In fact, red maple, a risk-adverse species, proved more sensitive to soil water content than red oak (Figure 3 and Figure 4). Coupled with the xylem isotope analysis, these results indicate that during conditions typical to a hydrologically regular year, the rooting strategy of red oaks offsets and may overcome the risks associated with its leaf and xylem hydraulic traits. Due to deeper root water uptake, red oaks are able to maintain steady transpiration rates during dry periods. Red maples, which rely more on ephemeral surficial soil waters and employ risk-adverse xylem and leaf traits, are unable to meet the levels of Ψ_L required for maintaining high transpiration rates by the isohydric stomatal strategy when soil moisture is low. Therefore, red maples close stomata in response to high VPD and suffer depleted stem water storage in dry inter-storm periods.

Traits along each of the three axes of the whole-plant hydraulic strategy (i.e., leaf, stem, and root) synergistically control stomatal conductance and thus both transpiration and photosynthesis. Over a long timescale, these factors affect plant growth and survival. In our site, the deep rooting strategy of red oaks increases the ability to endure short-term (days–weeks) water stress without catastrophic loss of conductivity or reductions in growth. Red oaks demonstrated no correlation between incremental annual bole growth and mean annual soil moisture at 30 cm, but red maple displayed a strong correlation (Figure 7). Bole growth was not correlated with mean growing season soil moisture, which may relate to the complex climatological and ecological significance of the winter precipitation (Reinmann & Templer, 2016) and to the uneven distribution of bole growth throughout the growing season (Jackson, 1952). Nonetheless, our growth analysis results demonstrate that red maple growth responds to soil water status at shallow depths, but oak growth does not. The carbon starvation hypothesis posed by McDowell et al. (2008) states that anisohydric species are susceptible to extreme drought due to hydraulic failure, but isohydric species will experience mortality during a prolonged drought due to limitations on carbon uptake imposed by tight stomatal control. The correlation between soil moisture and growth in the isohydric, but not the anisohydric species, supports this hypothesis. The additional drought tolerance afforded to red oak through its rooting strategy makes it less vulnerable to hydraulic failure than hypothesized on the basis of its stomatal regulation strategy and xylem architecture. This result highlights the importance of a synergistic, whole-tree approach to the study of tree hydrodynamics and their role in drought mortality. Ecologically, the combination of deep or efficient roots, highly conductive hydraulic tissues, and anisohydric stomatal strategy may be important for drought tolerance particularly in arid and semiarid regions (Brooks, Barnard, Coulombe, & McDonnell, 2010; Miller et al., 2010). Shallow roots, isohydric stomatal regulation, and less-conductive wood may be traits of species that are highly competitive in relatively wet places and during periods of high surface soil moisture, although avoiding stress when soil moisture availability is low.

Results from the sensitivity analysis demonstrated that traits at each organ level play a defining role in shaping intradaily transpiration dynamics, as well as the transpiration response to drying soil (Figure 8). The diversity in the magnitude and the diurnal pattern generated by each of the trait combinations affirm the importance of using a whole-plant framework to characterize plant hydraulic strategy rather than a single axis. We emphasize that our sensitivity analysis did not aim to reproduce our sap flux results, and there are similarities and differences between observed sap flux and the transpiration sensitivity test simulations for the suites of traits that match most closely with traits observed for red oak (simulation case 1) and red maple (simulation case 8). Similarly to the measured oak sap flux during the mini-drought (Figure 3), the simulated transpiration from simulation case 1 (Figure 8) showed limited skewness towards the morning hours and no decline across the 7-day simulation period. In contrast to the observed sap flux data in which sap flux from red maple exceeded that of red oak during non-limiting soil conditions (Figure 3), the magnitude of simulation case 1 consistently exceeded that of simulation case 8 (most similar to red maple, Figure 8) as well as that of simulation case 4 (isohydric, diffuse-porous, and deep roots, Figure 8), which could be considered analogous to a constantly well-watered red maple. As in the sap flux data recorded for maple, transpiration from simulation case 8 (Figure 8) declined steadily with declining soil water availability to near zero with a distinct skew towards the morning hours. Diurnal skewness is most pronounced during the least dry days of the simulation (days 1 and 2) and becomes increasingly smaller as overall transpiration declines. Observed sap flux, on the other hand, manifests the skew most strongly when the soil is driest (DOYs 221 and 222, Figure 3).

This skewed shape of diurnal transpiration depends on the stomatal response to VPD as well as the use of stem-stored water for transpiration early in the day and is partially responsible for the diurnal hysteresis of transpiration (Novick, Brantley, Miniat, Walker, & Vose, 2014; Zhang, Manzoni, Katul, Porporato, & Yang, 2014; Matheny et al., 2014b). This hysteresis has been hypothesized to be the source of missed intradaily dynamics of latent heat flux as simulated by land-surface models (LSMs) (Matheny et al., 2014a). Current LSMs cluster species into plant functional types (PFTs), which characterize trees by phenology, leaf traits, and bioclimatic limits, but do not explicitly represent hydraulic properties (Matheny et al., 2016; Quillet, Peng, & Garneau, 2010; Yang, Zhu, Peng, Wang, & Chen, 2015). For example, red oaks and red maples are often assigned to the same PFT (temperate deciduous broadleaf), despite their distinct patterns of water acquisition and use. As such, these models are prone to mischaracterize hydrologic cycling between the land surface and the atmosphere and are unlikely to simulate realistic ecosystem response to droughts, disturbances, or climate change (Link et al., 2014). Land-surface model representation of land-atmosphere water fluxes may be improved by replacing current PFT-based parameterizations with new parameterizations that account for variability in whole-plant hydraulic traits (Matheny et al., 2016). Alternatively, the incorporation of statistically scalable tree-level hydrodynamics models (e.g., Sperry et al., 1998; Bohrer et al., 2005; Janott et al., 2011; Gentine, Guérin, Uriarte, McDowell, & Pockman, 2015; Mirfenderesgi et al., 2016) into existing LSM schemes will permit leaf, stem, and root-level traits to be accounted for directly. The work of Xu et al. (2016) demonstrates this pathway for model improvement. Although this method to incorporate plant hydraulic strategies into LSMs will require increased model parameterization, tools such as the TRY Global Plant Trait Database (Kattge et al., 2011) and frameworks of ecosystem-level functional properties (Musavi et al., 2015) will facilitate the effort.

5 | CONCLUSION

The emergent phenotypical hydraulic traits at each of the root, stem, and leaf levels combine to form a whole-plant hydraulic strategy. This strategy shapes interdaily and intradaily patterns of water flux, which contribute to long-term patterns of growth and individual responses to microclimate. The outcomes of these species-specific behaviors may remain unresolved by current modeling frameworks due to the over-aggregation of hydraulically dissimilar species into the same functional class. We therefore advocate the incorporation of more physically and structurally realistic plant hydraulics sub-models into larger land-surface and ecosystem models. These plant hydraulics models, such as FETCH2, will replace the current empirical link between soil moisture and stomatal conductance with mechanistic representations of stomatal response to stem, branch, or leaf water potential. Our results suggest that improving model parameterizations in this manner will be critical for improving simulations of ecosystem responses to drought and other changes to canopy structure, forest composition, and climate. Increased accuracy in model representations of transpiration and the combination of traits that control it will translate directly into better predictions of growth and mortality, as well as improved simulations of the terrestrial surface energy budget and global carbon and water balances.

ACKNOWLEDGEMENTS

Funding for this study was provided by the U.S. Department of Energy's Office of Science, Office of Biological and Environmental Research, Terrestrial Ecosystem Sciences Program Award Grant DE-SC0007041 and Ameriflux Management program under Flux Core Site Agreement Grant 7096915 through Lawrence Berkeley National Laboratory and the National Science Foundation Hydrological Science Grant 1521238. Support for A.M.M. was provided by The Ohio State University Presidential Fellowship and the P.E.O. Scholar Award. R.P.F. received support from NSF Graduate Research Fellowship Grant 2011094378. Any opinions, findings, and conclusions or recommendations expressed in this material are those of the authors and do not necessarily reflect the views of the funding agencies.

CONFLICT OF INTEREST

The authors have no conflicts of interest to declare.

REFERENCES

Abrams, M. D. (1990). Adaptations and responses to drought in *Quercus* species of North America. *Tree Physiology*, *7*, 227–238.

Allen, M. F. (2009). Water relations in the mycorrhizosphere. In U. Luttge, W. Beyschlag, B. Budel, & D. Francis (Eds.), *Progress in Botany* (pp. 257–276). Berlin & Heidelberg, Germany: Springer-Verlag.

Attia, Z., Domec, J. C., Oren, R., Way, D. A., & Moshelion, M. (2015). Growth and physiological responses of isohydric and anisohydric poplars to drought. *Journal of Experimental Botany*. doi:10.1093/jxb/erv195

Baldocchi, D. D., & Xu, L. K. (2007). What limits evaporation from Mediterranean oak woodlands–the supply of moisture in the soil, physiological control by plants or the demand by the atmosphere? *Advances in Water Resources*, *30*, 2113–2122. doi:10.1016/j.advwatres.2006.06.013

Barnes, C. J., & Allison, G. B. (1988). Tracing of water movement in the unsaturated zone using stable isotopes of hydrogen and oxygen. *Journal of Hydrology*, *100*, 143–176. doi:10.1016/0022-1694(88)90184-9

Barnes, C. J., & Turner, J. V. (1998). Isotopic Exchange in Soil Water. In C. McDonnell, & J. J. Kendall (Eds.), *Isotope Tracers in Catchment Hydrology* (pp. 137–163). Amsterdam: Elsevier.

Berkelhammer, M., Hu, J., Bailey, A., Noone, D. C., Still, C. J., Barnard, … Turnipseed, A. (2013). The nocturnal water cycle in an open-canopy forest. *Journal of Geophysical Research-Atmospheres*, *118*, 10225–10242.

Bohrer, G., Mourad, H., Laursen, T. A., Drewry, D., Avissar, R., Poggi, D., … Katul, G. G. (2005). Finite element tree crown hydrodynamics model (FETCH) using porous media flow within branching elements: A new representation of tree hydrodynamics. *Water Resources Research*, *41*. doi:10.1029/2005wr004181

Bovard, B. D., Curtis, P. S., Vogel, C. S., Su, H.-B., & Schmid, H. P. (2005). Environmental controls on sap flow in a northern hardwood forest. *Tree Physiology*, *25*, 31–38.

Breecker, D. O., Sharp, Z. D., & McFadden, L. D. (2009). Seasonal bias in the formation and stable isotopic composition of pedogenic carbonate in modem soils from central New Mexico, USA. *Geological Society of America Bulletin*, *121*, 630–640. doi:10.1130/b26413.1

Brooks, R. J., Barnard, H. R., Coulombe, R., & McDonnell, J. J. (2010). Ecohydrologic separation of water between trees and streams in a Mediterranean climate. *Nature Geoscience*, *3*, 100–104.

Canadell, J., Jackson, R. B., Ehleringer, J. R., Mooney, H. A., Sala, O. E., & Schulze, E. D. (1996). Maximum rooting depth of vegetation types at the global scale. *Oecologia*, *108*, 583–595. doi:10.1007/bf00329030

Canadell, J. G., Pataki, D. E., & Pitelka, L. (2007). *Terrestrial ecosystems in a changing world*, Springer, Berlin. New: York.

Choat, B., Jansen, S., Brodribb, T. J., Cochard, H., Delzon, S., Bhaskar, R., … Zanne, A. E. (2012). Global convergence in the vulnerability of forests to drought. *Nature*, *491*, 752–756. doi:10.1038/nature11688

Clearwater, M. J., Meinzer, F. C., Andrade, J. L., Goldstein, G., & Holbrook, N. M. (1999). Potential errors in measurement of nonuniform sap flow using heat dissipation probes. *Tree Physiology*, *19*, 681–687.

Cochard, H., Breda, N., Granier, A., & Aussenac, G. (1992). Vulnerability to air-embolism of three European oak species (*Quercus petraea* (Matt) Liebl, *Q pubescens* Willd, *Q robur* L). *Annales des Sciences Forestières*, *49*, 225–233. doi:10.1051/forest:19920302

Coplen, T. B. (1996). New guidelines for reporting stable hydrogen, carbon, and oxygen isotope-ratio data. *Geochimica et Cosmochimica Acta*, *60*, 3359–3360. doi:10.1016/0016-7037(96)00263-3

Craig, H. (1961). Standard for reporting concentrations of deuterium and oxygen-18 in natural waters. *Science*, *133*. doi:10.1126/science.133.3467.1833.1833-&

Dansgaard, W. (1964). Stable isotopes in precipitation. *Tellus*, *16*, 436–468.

Dawson, T. E. (1993). Hydraulic lift and water use by plants: Implications for water balance, performance and plant-plant interactions. *Oecologia*, *95*, 565–574.

Dawson, T. E. (1996). Determining water use by trees and forests from isotopic, energy balance and transpiration analyses: The roles of tree size and hydraulic lift. *Tree Physiology*, *16*, 263–272.

Dawson, T. E., & Simonin, K. A. (2011). The roles of stable isotopes in forest hydrology and biogeochemistry. In D. F. Levia, D. Carlyle-Moses, & T. Tanaka (Eds.), *Forest Hydrology and Biogeochemistry* (pp. 137–161) Springer Netherlands.

Ehleringer, J. R., & Dawson, T. E. (1992). Water uptake by plants: Perspectives from stable isotope composition. *Plant, Cell & Environment*, *15*, 1073–1082. doi:10.1111/j.1365-3040.1992.tb01657.x

Ehleringer, J. R., Roden, J., & Dawson, T. E. (2000). Assessing ecosystem-level water relations through stable isotope ratio analyses. In O. E. Sala, R. B. Jasckson, H. A. Mooney & R. Howarth (Eds.), *Methods in Ecosystem Science* (pp. 181–198). New York: Springer-Verlag.

Ford, C. R., Hubbard, R. M., & Vose, J. M. (2011). Quantifying structural and physiological controls on variation in canopy transpiration among planted pine and hardwood species in the southern Appalachians. *Ecohydrology*, *4*, 183–195. doi:10.1002/eco.136

Friedman, I., Harris, J. M., Smith, G. I., & Johnson, C. A. (2002). Stable isotope composition of waters in the Great Basin, United States 1. Air-mass trajectories. *Journal of Geophysical Research-Atmospheres*, *107*, 14. doi:10.1029/2001jd000565

Gaines, K. P., Stanley, J. W., Meinzer, F. C., McCulloh, K. A., Woodruff, D. R., Chen, W., … Eissenstat, D. M. (2015). Reliance on shallow soil water in a mixed-hardwood forest in central Pennsylvania. *Tree Physiology*. doi:10.1093/treephys/tpv113

Gao, J. G., Zhao, P., Shen, W. J., Niu, J. F., Zhu, L. W., & Ni, G. Y. (2015). Biophysical limits to responses of water flux to vapor pressure deficit in seven tree species with contrasting land use regimes. *Agricultural and Forest Meteorology*, *200*, 258–269. doi:10.1016/j.agrformet.2014.10.007

Gat, J. R. (1996). Oxygen and hydrogen isotopes in the hydrologic cycle. *Annual Review of Earth and Planetary Sciences*, *24*, 225–262. doi:10.1146/annurev.earth.24.1.225

Gazis, C., & Feng, X. H. (2004). A stable isotope study of soil water: Evidence for mixing and preferential flow paths. *Geoderma*, *119*, 97–111. doi:10.1016/s0016-7061(03)00243-x

Gentine, P., Guérin, M., Uriarte, M., McDowell, N. G., & Pockman, W. T. (2015). An allometry-based model of the survival strategies of hydraulic failure and carbon starvation. *Ecohydrology*. doi:10.1002/eco.1654

Gleason, S. M., Westoby, M., Jansen, S., Choat, B., Hacke, U. G., Pratt, R. B., … Zanne, A. E. (2016). Weak tradeoff between xylem safety and xylem-specific hydraulic efficiency across the world's woody plant species. *The New Phytologist*, *209*, 123–136. doi:10.1111/nph.13646

Gough, C. M., & Curtis, P. S. (1999). AmeriFlux US-UMB Univ. of Mich. Biological Station. *Dataset*. doi:10.17190/AMF/1246107.

Gough, C. M., Hardiman, B. S., Nave, L. E., Bohrer, G., Maurer, K. D., Vogel, C. S., … Curtis, P. S. (2013). Sustained carbon uptake and storage following moderate disturbance in a Great Lakes forest. *Ecological Applications*, *23*, 1202–1215. doi:10.1890/12-1554.1

Gough, C. M., Vogel, C. S., Hardiman, B., & Curtis, P. S. (2010). Wood net primary production resilience in an unmanaged forest transitioning from early to middle succession. *Forest Ecology and Management*, *260*, 36–41. doi:10.1016/j.foreco.2010.03.027

Granier, A. (1985). A new method of sap flow measurement in tree stems. *Annales des Sciences Forestières*, *42*, 193–200. doi:10.1051/forest:19850204

Granier, A. (1987). Evaluation of transiration in a Douglas-fir stand by means of sap flow measurements. *Tree Physiology*, *3*, 309–319.

Gu, L., Pallardy, S. G., Hosman, K. P., & Sun, Y. (2015). Drought-influenced mortality of tree species with different predawn leaf water dynamics in a decade-long study of a central US forest. *Biogeosciences*, *12*, 2831–2845. doi:10.5194/bg-12-2831-2015

Gupta, P., Noone, D., Galewsky, J., Sweeney, C., & Vaughn, B. H. (2009). Demonstration of high-precision continuous measurements of water vapor isotopologues in laboratory and remote field deployments using wavelength-scanned cavity ring-down spectroscopy (WS-CRDS) technology. *Rapid Communications in Mass Spectrometry*, *23*, 2534–2542.

He, L. L., Ivanov, V. Y., Bohrer, G., Thomsen, J. E., Vogel, C. S., & Moghaddam, M. (2013). Temporal dynamics of soil moisture in a northern temperate mixed successional forest after a prescribed intermediate disturbance. *Agricultural and Forest Meteorology*, *180*, 22–33. doi:10.1016/j.agrformet.2013.04.014

Hernandez-Santana, V., Martinez-Fernandez, J., Moran, C., & Cano, A. (2008). Response of *Quercus pyrenaica* (melojo oak) to soil water deficit: A case study in Spain. *European Journal of Forest Research*, *127*, 369–378. doi:10.1007/s10342-008-0214-x

Horton, J. L., & Hart, S. C. (1998). Hydraulic lift: A potentially important ecosystem process. *Trends in Ecology & Evolution*, *13*, 232–235. doi:10.1016/s0169-5347(98)01328-7

Jackson, L. W. R. (1952). Radial growth of forest trees in the Georgia Piedmont. *Ecology*, *33*, 336–341. doi:10.2307/1932829

Jackson, R. B., Canadell, J., Ehleringer, J. R., Mooney, H. A., Sala, O. E., & Schulze, E. D. (1996). A global analysis of root distributions for terrestrial biomes. *Oecologia*, *108*, 389–411. doi:10.1007/Bf00333714

Janott, M., Gayler, S., Gessler, A., Javaux, M., Klier, C., & Priesack, E. (2011). A one-dimensional model of water flow in soil-plant systems based on plant architecture. *Plant and Soil*, *341*, 233–256. doi:10.1007/s11104-010-0639-0

Kattge, J., Diaz, S., Lavorel, S., Prentice, C., Leadley, P., Bonisch, G., … Wirth, C. (2011). TRY–a global database of plant traits. *Global Change Biology*, *17*, 2905–2935. doi:10.1111/j.1365-2486.2011.02451.x

Kocher, P., Horna, V., & Leuschner, C. (2013). Stem water storage in five coexisting temperate broad-leaved tree species: Significance, temporal dynamics and dependence on tree functional traits. *Tree Physiology*, *33*, 817–832. doi:10.1093/treephys/tpt055

Link, P., Simonin, K., Maness, H., Oshun, J., Dawson, T., & Fung, I. (2014). Species differences in the seasonality of evergreen tree transpiration in a Mediterranean climate: Analysis of multiyear, half-hourly sap flow observations. *Water Resources Research*, *50*, 1869–1894. doi:10.1002/2013wr014023

Maherali, H., Moura, C. F., Caldeira, M. C., Willson, C. J., & Jackson, R. B. (2006). Functional coordination between leaf gas exchange and vulnerability to xylem cavitation in temperate forest trees. *Plant, Cell & Environment*, *29*, 571–583. doi:10.1111/j.1365-3040.2005.01433.x

Manzoni, S. (2014). Integrating plant hydraulics and gas exchange along the drought-response trait spectrum. *Tree Physiology*, *34*, 1031–1034. doi:10.1093/treephys/tpu088

Manzoni, S., Vico, G., Katul, G., Palmroth, S., & Porporato, A. (2014). Optimal plant water-use strategies under stochastic rainfall. *Water Resources Research*, *50*, 5379–5394. doi:10.1002/2014WR015375

Manzoni, S., Vico, G., Katul, G. G., Palmroth, S., Jackson, R. B., & Porporato, A. (2013). Hydraulic limits on maximum plant transpiration and the emergence of the safety–efficiency trade-off. *The New Phytologist*. doi:10.1111/nph.12126

Martinez-Vilalta, J., Poyatos, R., Aguade, D., Retana, J., & Mencuccini, M. (2014). A new look at water transport regulation in plants. *The New Phytologist*, *204*, 105–115. doi:10.1111/nph.12912

Matheny, A. M., Bohrer, G., Garrity, S. R., Morin, T. H., Howard, C. J., & Vogel, C. S. (2015). Observations of stem water storage in trees of opposing hydraulic strategies. *Ecosphere*, *6*, 165. doi:10.1890/ES15-00170.1

Matheny, A. M., Bohrer, G., Stoy, P. C., Baker, I., Black, A. T., Desai, A. R., … Verbeeck, H. (2014a). Characterizing the diurnal patterns of errors in the prediction of evapotranspiration by several land-surface models: An NACP analysis. *Journal of Geophysical Research*, *119*, 1458–1473. doi:10.1002/2014JG002623

Matheny, A. M., Bohrer, G., Vogel, C. S., Morin, T. H., He, L., Frasson, R. P. M., … Curtis, P. S. (2014b). Species-specific transpiration responses to intermediate disturbance in a northern hardwood forest. *Journal of Geophysical Research*, *119*, 2292–2311. doi:10.1002/2014JG002804

Matheny, A. M., Mirfenderesgi, G., & Bohrer, G. (2016). Trait-based representation of hydrological functional properties of plants in weather and ecosystem models. *Plant Diversity*, In press. doi:10.1016/j.pld.2016.10.001

Matthes, J. H., Goring, S., Williams, J. W., & Dietze, M. C. (2016). Benchmarking historical CMIP5 plant functional types across the Upper Midwest and Northeastern United States. *Journal of Geophysical Research*, 2015JG003175. doi:10.1002/2015JG003175

Maurer, K. D., Hardiman, B. S., Vogel, C. S., & Bohrer, G. (2013). Canopy-structure effects on surface roughness parameters: Observations in a Great Lakes mixed-deciduous forest. *Agricultural and Forest Meteorology*, *177*, 24–34. doi:10.1016/j.agrformet.2013.04.002

McCulloh, K. A., Johnson, D. M., Meinzer, F. C., Voelker, S. L., Lachenbruch, B., & Domec, J.-C. (2012). Hydraulic architecture of two species differing in wood density: Opposing strategies in co-occurring tropical pioneer trees. *Plant, Cell & Environment*, *35*, 116–125. doi:10.1111/j.1365-3040.2011.02421.x

McDowell, N., Pockman, W. T., Allen, C. D., Breshears, D. D., Cobb, N., Kolb, T., … Yepez, E. A. (2008). Mechanisms of plant survival and mortality during drought: Why do some plants survive while others succumb to drought? *The New Phytologist*, *178*, 719–739. doi:10.1111/j.1469-8137.2008.02436.x

Meinzer, F. C., Andrade, J. L., Goldstein, G., Holbrook, N. M., Cavelier, J., & Wright, S. J. (1999). Partitioning of soil water among canopy trees in a seasonally dry tropical forest. *Oecologia*, *121*, 293–301. doi:10.1007/s004420050931

Meinzer, F. C., McCulloh, K. A., Lachenbruch, B., Woodruff, D. R., & Johnson, D. M. (2010). The blind men and the elephant: The impact of context and scale in evaluating conflicts between plant hydraulic safety and efficiency. *Oecologia*, *164*, 287–296. doi:10.1007/s00442-010-1734-x

Meinzer, F. C., Woodruff, D. R., Eissenstat, D. M., Lin, H. S., Adams, T. S., & McCulloh, K. A. (2013). Above- and belowground controls on water use by trees of different wood types in an eastern US deciduous forest. *Tree Physiology*, *33*, 345–356. doi:10.1093/treephys/tpt012

Meinzer, F. C., Woodruff, D. R., Marias, D. E., McCulloh, K. A., & Sevanto, S. (2014). Dynamics of leaf water relations components in co-occurring iso-and anisohydric conifer species. *Plant, Cell & Environment*, *37*, 2577–2586. doi:10.1111/pce.12327

Miller, G. R., Chen, X. Y., Rubin, Y., Ma, S. Y., & Baldocchi, D. D. (2010). Groundwater uptake by woody vegetation in a semiarid oak savanna. *Water Resources Research*, *46*, 14. doi:10.1029/2009wr008902

Mirfenderesgi, G., Bohrer, G., Matheny, A. M., Fatichi, S., Frasson, R. P. M., & Schäfer, K. V. R. (2016). Tree level hydrodynamic approach for resolving aboveground water storage and stomatal conductance and modeling the effects of tree hydraulic strategy. *Journal of Geophysical Research: Biogeosciences*, 1792–1813.

Musavi, T., Mahecha, M. D., Migliavacca, M., Reichstein, M., van de Weg, M. J., van Bodegom, P. M., … Kattge, J. (2015). The imprint of plants on ecosystem functioning: A data-driven approach. *International Journal of Applied Earth Observation and Geoinformation*, *43*, 119–131. doi:10.1016/j.jag.2015.05.009

Nadezhdina, N., Ferreira, M. I., Silva, R., & Pacheco, C. A. (2008). Seasonal variation of water uptake of a *Quercus suber* tree in Central Portugal. *Plant and Soil*, *305*, 105–119. doi:10.1007/s11104-007-9398-y

Nave, L. E., Gough, C. M., Maurer, K. D., Bohrer, G., Hardiman, B. S., Le Moine, J., … Curtis, P. S. (2011). Disturbance and the resilience of coupled carbon and nitrogen cycling in a north temperate forest. *Journal of Geophysical Research*, *116*. doi:10.1029/2011jg001758

Nolf, M., Creek, D., Duursma, R., Holtum, J., Mayr, S., & Choat, B. (2015). Stem and leaf hydraulic properties are finely coordinated in three tropical rainforest tree species. *Plant, Cell & Environment*. doi:10.1111/pce.12581

Novick, K., Brantley, S., Miniat, C. F., Walker, J., & Vose, J. M. (2014). Inferring the contribution of advection to total ecosystem scalar fluxes over a tall forest in complex terrain. *Agricultural and Forest Meteorology*, *185*, 1–13. doi:10.1016/j.agrformet.2013.10.010

Novick, K. A., Miniat, C. F., & Vose, J. M. (2015). Drought limitations to leaf-level gas exchange: Results from a model linking stomatal optimization and cohesion–tension theory. *Plant, Cell & Environment*. doi:10.1111/pce.12657

Oishi, A. C., Oren, R., & Stoy, P. C. (2008). Estimating components of forest evapotranspiration: A footprint approach for scaling sap flux measurements. *Agricultural and Forest Meteorology*, *148*, 1719–1732. doi:10.1016/j.agrformet.2008.06.013

Oren, R., & Pataki, D. E. (2001). Transpiration in response to variation in microclimate and soil moisture in southeastern deciduous forests. *Oecologia*, *127*, 549–559. doi:10.1007/s004420000622

Phillips, S. L., & Ehleringer, J. R. (1995). Limited uptake of summer precipitation by bigtooth maple (*Acer grandidentatum* Nutt) and Gambel's oak (*Quereus gambelii* Nutt). *Trees*, *9*, 214–219. doi:10.1007/bf00195275

Pinto, C. A., Nadezhdina, N., David, J. S., Kurz-Besson, C., Caldeira, M. C., Henriques, M. O., … David, T. S. (2014). Transpiration in *Quercus suber* trees under shallow water table conditions: The role of soil and groundwater. *Hydrological Processes*, *28*, 6067–6079. doi:10.1002/hyp.10097

Pockman, W. T., & Sperry, J. S. (2000). Vulnerability to xylem cavitation and the distribution of Sonoran desert vegetation. *American Journal of Botany*, *87*, 1287–1299. doi:10.2307/2656722

Poulter, B., Ciais, P., Hodson, E., Lischke, H., Maignan, F., Plummer, S., & Zimmermann, N. E. (2011). Plant functional type mapping for earth system models. *Geoscientific Model Development*, *4*, 993–1010. doi:10.5194/gmd-4-993-2011

Quillet, A., Peng, C. H., & Garneau, M. (2010). Toward dynamic global vegetation models for simulating vegetation-climate interactions and feedbacks: Recent developments, limitations, and future challenges. *Environmental Reviews*, *18*, 333–353. doi:10.1139/a10-016

Rawls, W. J., Brakensiek, D. L., & Saxton, K. E. (1982). Estimation of soil water properties. *Transactions of ASAE*, *25*, 1316–1328.

Reinmann, A. B., & Templer, P. H. (2016). Reduced winter snowpack and greater soil frost reduce live root biomass and stimulate radial growth and stem respiration of red maple (*Acer rubrum*) trees in a mixed-hardwood forest. *Ecosystems*, *19*, 129–141. doi:10.1007/s10021-015-9923-4

Roman, D. T., Novick, K. A., Brzostek, E. R., Dragoni, D., Rahman, F., & Phillips, R. P. (2015). The role of isohydric and anisohydric species in determining ecosystem-scale response to severe drought. *Oecologia*, 1–14. doi:10.1007/s00442-015-3380-9

Scholl, M. A., Ingebritsen, S. E., Janik, C. J., & Kauahikaua, J. P. (1996). Use of precipitation and groundwater isotopes to interpret regional hydrology on a tropical volcanic island: Kilauea volcano area, Hawaii. *Water Resour. Res.*, *32*, 3525–3537. doi:10.1029/95wr02837

Simonin, K. A., Link, P., Rempe, D., Miller, S., Oshun, J., Bode, C., … Dawson, T. E. (2014). Vegetation induced changes in the stable isotope composition of near surface humidity. *Ecohydrology*, *7*, 936–949. doi:10.1002/eco.1420

Skelton, R. P., West, A. G., & Dawson, T. E. (2015). Predicting plant vulnerability to drought in biodiverse regions using functional traits. *Proceedings of the National Academy of Sciences*, *112*, 5744–5749. doi:10.1073/pnas.1503376112

Sperry, J. S., Adler, F. R., Campbell, G. S., & Comstock, J. P. (1998). Limitation of plant water use by rhizosphere and xylem conductance: Results from a model. *Plant, Cell & Environment*, *21*, 347–359. doi:10.1046/j.1365-3040.1998.00287.x

Sperry, J. S., Nichols, K. L., Sullivan, J. E. M., & Eastlack, S. E. (1994). Xylem embolism in ring-porous, diffuse-porous and coniferous trees of northern Utah and interior Alaska. *Ecology*, *75*, 1736–1752. doi:10.2307/1939633

Thomsen, J., Bohrer, G., Matheny, A. M., Ivanov, V. Y., He, L., Renninger, H., & Schäfer, K. (2013). Contrasting hydraulic strategies during dry soil conditions in *Quercus rubra* and *Acer rubrum* in a sandy site in Michigan. *Forests*, *4*, 1106–1120.

Tognetti, R., Longobucco, A., & Raschi, A. (1998). Vulnerability of xylem to embolism in relation to plant hydraulic resistance in *Quercus pubescens* and *Quercus ilex* co-occurring in a Mediterranean coppice stand in central Italy. *The New Phytologist*, *139*, 437–447. doi:10.1046/j.1469-8137.1998.00207.x

Tremoy, G., Vimeux, F., Cattani, O., Mayaki, S., Souley, I., & Favreau, G. (2011). Measurements of water vapor isotope ratios with wavelength-scanned cavity ring-down spectroscopy technology: new insights and important caveats for deuterium excess measurements in tropical areas in comparison with isotope-ratio mass spectrometry. *Rapid Communications in Mass Spectrometry*, *25*, 3469–3480.

Van Genuchten, M. T. (1980). A closed-form equation for predicting the hydraulic conductivity of unsaturated soils. *Soil Science Society of America Journal*, *44*, 892–898.

von Allmen, E. I., Sperry, J. S., & Bush, S. E. (2014). Contrasting whole-tree water use, hydraulics, and growth in a co-dominant diffuse-porous vs. ring-porous species pair. *Trees*, 1–12. doi:10.1007/s00468-014-1149-0

West, A. G., Dawson, T. E., February, E. C., Midgley, G. F., Bond, W. J., & Aston, T. L. (2012). Diverse functional responses to drought in a Mediterranean-type shrubland in South Africa. *The New Phytologist*, *195*, 396–407. doi:10.1111/j.1469-8137.2012.04170.x

Walker, C. D., & Richardson, S. B. (1991). The use of stable isotopes of water in characterizing the source of water in vegetation. *Chemical Geology*, *94*, 145–158.

West, A. G., Goldsmith, G. R., Matimati, I., & Dawson, T. E. (2011). Spectral analysis software improves confidence in plant and soil water stable isotope analyses performed by isotope ratio infrared spectroscopy (IRIS). *Rapid Communications in Mass Spectrometry*, *25*, 2268–2274. doi:10.1002/rcm.5126

Wullschleger, S. D., Hanson, P. J., & Todd, D. E. (1996). Measuring stem water content in four deciduous hardwoods with a time-domain reflectometer. *Tree Physiology*, *16*, 809–815.

Wullschleger, S. D., Meinzer, F. C., & Vertessy, R. A. (1998). A review of whole-plant water use studies in tree. *Tree Physiology*, *18*, 499–512.

Xu, X., Medvigy, D., Powers, J. S., Becknell, J. M., & Guan, K. (2016). Diversity in plant hydraulic traits explains seasonal and inter-annual variations of vegetation dynamics in seasonally dry tropical forests. *The New Phytologist*. doi:10.1111/nph.14009

Yang, Y. Z., Zhu, Q. A., Peng, C. H., Wang, H., & Chen, H. (2015). From plant functional types to plant functional traits A new paradigm in modelling global vegetation dynamics. *Progress in Physical Geography*, *39*, 514–535. doi:10.1177/0309133315582018

Zhang, Q., Manzoni, S., Katul, G. G., Porporato, A., & Yang, D. (2014). The hysteretic evapotranspiration—Vapor pressure deficit relation. *Journal of Geophysical Research*, *119*, 125–140. doi:10.1002/2013JG002484

How to cite this article: Matheny AM, Fiorella RP, Bohrer G, Poulsen CJ, Morin TH, Wunderlich A, Vogel CS, Curtis PS. Contrasting strategies of hydraulic control in two codominant temperate tree species. *Ecohydrology*. 2016; e1815. doi: 10.1002/eco.1815